iScience

CellPress

Article

Vitamin D/Vitamin D Receptor Signaling Is Required for Normal Development and Function of Group 3 Innate Lymphoid Cells in the Gut

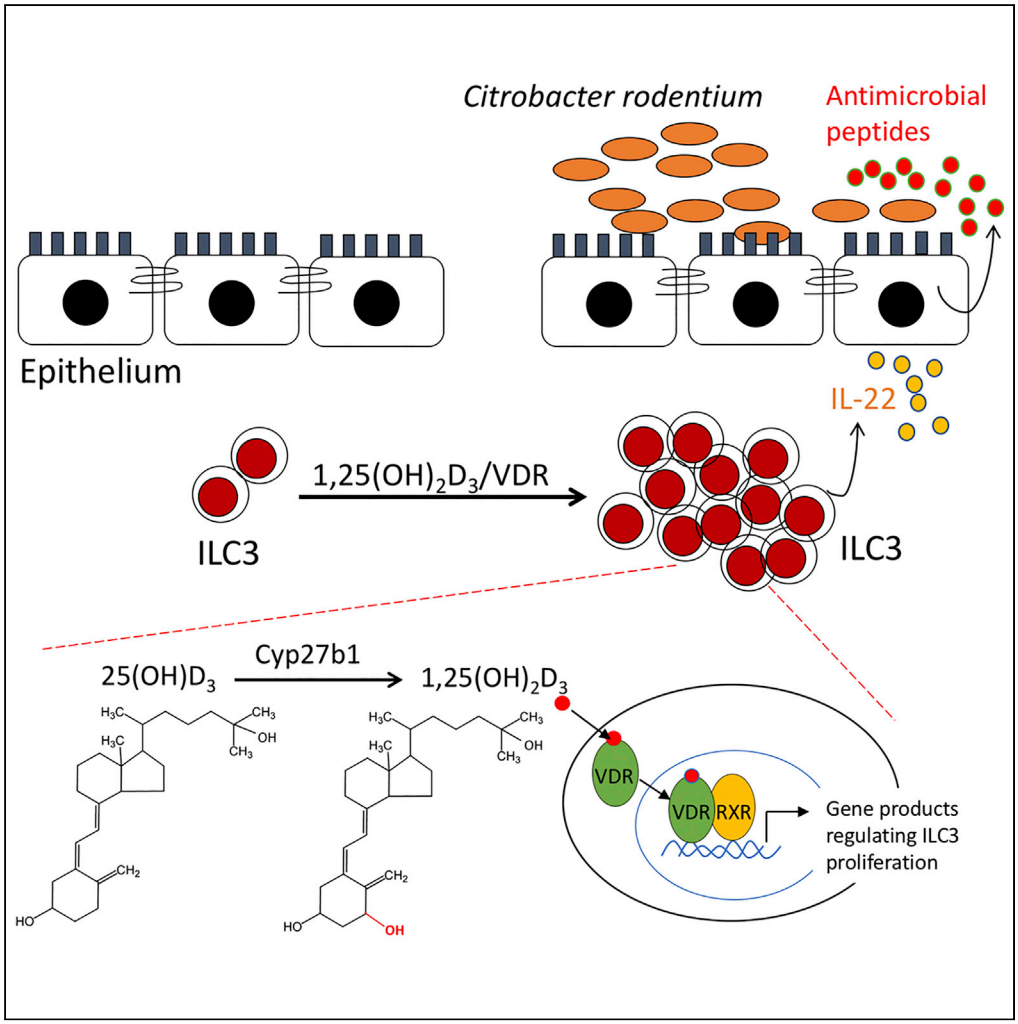

Lei He, Min Zhou, Yan Chun Li

cyan@medicine.bsd.uchicago.edu

HIGHLIGHTS

VDR or $1,25(OH)_2D_3$ deficiency reduces ILC3 populations and impairs ILC3 immunity

Vitamin D/VDR signaling is required for proper ILC3 proliferation

Vitamin D regulation of ILC3 is independent of T and B cells or gut microflora

He et al., iScience *17*, 119–131
July 26, 2019
https://doi.org/10.1016/j.isci.2019.06.026

iScience

CellPress

Article

Vitamin D/Vitamin D Receptor Signaling Is Required for Normal Development and Function of Group 3 Innate Lymphoid Cells in the Gut

Lei He,[1] Min Zhou,[1,2] and Yan Chun Li[1,3,*]

SUMMARY

Group 3 innate lymphoid cells (ILC3) play key roles in protective immunity and mucosal barrier maintenance. Here we showed that vitamin D/vitamin D receptor (VDR) signaling regulates gut ILC3. VDR deletion or 1,25-dihydroxyvitamin D deficiency in mice led to a marked reduction in colonic ILC3 populations at steady state and impaired ILC3 responses following *Citrobacter rodentium* infection, resulting in substantial increases in intestinal bacterial growth and mouse mortality. VDR regulation of ILC3 was independent of T and B lymphocytes or gut microflora. Correction of 1,25-dihydroxyvitamin D deficiency rescued the ILC3 defects. Mechanistically, VDR deletion or 1,25-dihydroxyvitamin D deficiency markedly reduced colonic Ki67$^+$ ILC3 populations, and *in vivo* and *in vitro* studies confirmed that vitamin D hormone directly stimulated ILC3 proliferation. Therefore, vitamin D/VDR signaling is required for ILC3-mediated innate immunity through regulation of ILC3 proliferation.

INTRODUCTION

The vitamin D hormone is a major endocrine system with pleiotropic functions (Bouillon et al., 2008). Physiologically, the majority of the body's vitamin D content is derived from photosynthesis in the skin following UV irradiation, and thus body's vitamin D levels are influenced by geographic locations, seasonal changes, and skin pigmentations (Holick, 2007, 2018). Vitamin D is converted to the active hormone 1,25-dihydroxyvitamin D ($1,25(OH)_2D_3$) by two steps of hydroxylation: 25-hydroxylation in the liver followed by 1α-hydroxylation in the kidney (Holick, 1996). Cyp27b1 (25-hydroxyvitamin D 1α-hydroxylase) is the rate-limiting enzyme required for the synthesis of $1,25(OH)_2D_3$. The biological activities of $1,25(OH)_2D_3$ is mediated by the vitamin D receptor (VDR), a nuclear hormone receptor (Haussler et al., 2013). The gut is one of the tissues in the body that have the most abundant VDR expression (Wang et al., 2012), indicating that it is a major physiological target of vitamin D. It is long established that vitamin D/VDR signaling regulates duodenal transcellular calcium transport (Lee et al., 2015). Recent studies demonstrated that gut epithelial VDR plays a key role in protecting the mucosal barrier integrity (He et al., 2018; Liu et al., 2013). However, little is known about the effect of vitamin D/VDR signaling on the immune components of the gut, including the gut innate immunity.

Innate lymphoid cells (ILCs) are a set of newly discovered innate immune cells emerging as crucial effectors of innate immunity in diverse physiological functions including host defense against infection, tissue remodeling, and maintenance of mucosal barrier integrity (Artis and Spits, 2015; Bernink et al., 2013). The diverse populations of ILC family are characterized by a classic lymphoid cell morphology that lacks expression of somatically rearranged antigen receptors and lineage surface markers characteristic of myeloid origin or adaptive immune system; as such, ILCs do not exhibit any degree of antigen specificity and are lineage marker-negative cells (Artis and Spits, 2015). ILCs are derived from an Id2-dependent common lymphoid progenitor cell population and require interleukin (IL)-7 for their maintenance. ILCs can be grouped based on the transcription factors required for their development and function, and currently there are three major groups: T-bet$^+$ ILC (Group 1, ILC1), GATA3$^+$ ILC (Group 2, ILC2), and RORγt$^+$ ILC (Group 3, ILC3) (Artis and Spits, 2015; Sonnenberg and Artis, 2012).

RORγt$^+$ ILC3 is the major ILC in the gut that predominantly produces IL-22 and IL-17 and plays critical roles in protective immunity against bacteria (Sonnenberg and Artis, 2012). It is known that IL-22 stimulates epithelial cells to secret anti-microbial peptides, including RegIIIγ, lipocalin-2, and β-defensins, to constrain pathogenic bacterial growth (Wolk et al., 2004; Zheng et al., 2008). IL-22 also induces mucin expression and colonic epithelial cell proliferation to maintain the integrity of the mucosal barrier (Sugimoto et al., 2008). ILC3 is heterogeneous in mice and humans. In mice, two subsets can be distinguished

[1]Department of Medicine, Division of Biological Sciences, The University of Chicago, Chicago, IL 60637, USA

[2]Division of Gastroenterology, Xinhua Hospital, Shanghai Jiao Tong University School of Medicine, Shanghai 200092, China

[3]Lead Contact

*Correspondence: cyan@medicine.bsd.uchicago.edu

https://doi.org/10.1016/j.isci.2019.06.026

based on the expression of chemokine receptor CCR6. $CCR6^+$ ILC3 include $CD4^+$ and $CD4^-$ lymphoid tissue inducer (LTi) cells, namely, LTi4 and LTi0, and $CCR6^-$ ILC3 encompass cells that express natural cytotoxicity receptor NKp46, namely, $NKp46^+$ (or NK22) cells. The development of ILC3 is regulated by a number of nuclear hormone receptors, including $ROR\gamma t^+$, RARα, and AHR (Artis and Spits, 2015; Qiu et al., 2012; Sawa et al., 2010; Spencer et al., 2014). Moreover, the development of ILC2 and ILC3 in the gut is deeply influenced by micronutrients such as vitamin A (Spencer et al., 2014).

Vitamin D as a micronutrient is well known for its immune-modulatory activity (Hart et al., 2011; Mora et al., 2008). A body of research has demonstrated the importance of vitamin D in the regulation of classic innate immune cells (e.g., monocytes, macrophages, dendritic cells) (Liu et al., 2006; Penna and Adorini, 2000) and adaptive immune cells (e.g., T_H1, T_H17, T_{reg}, B cells) (Joshi et al., 2011; Lemire et al., 1985; Mora et al., 2008; Penna et al., 2005; Rigby et al., 1984; Shirakawa et al., 2008; von Essen et al., 2010); however, few studies have directly assessed the role of the vitamin D/VDR signaling in ILC biology. Here we present evidence to demonstrate that this signaling pathway is an important regulator of ILC3 development and is required for ILC3-mediated innate immunity in the gut.

RESULTS

Reduced Colonic ILC3 Populations in $VDR^{-/-}$ Mice

Our interest in ILC3 initially derived from an observation that gut ILC3 expressed a high level of VDR. We quantified by qRT-PCR the baseline *Vdr* transcript level in colonic ILC3 ($CD3^-CD90^{hi}CD45^{lo}$) (Guo et al., 2014) and T_H17 cells ($CD3^+CD4^+TCR\beta^+GFP(ROR\gamma t)^+$) that were sorted from colonic lamina propria (LP) cells by fluorescence-activated cell sorting (FACS) and found that ILC3 *Vdr* transcript was higher compared with sorted T_H17 cells or purified intestinal epithelial cells (Figure S1), suggesting a role of VDR in ILC3 biology. To address whether VDR regulates ILC3, we compared the colonic mucosal profiles of ILC3 and the sub-populations between $VDR^{-/-}$ and wild-type (WT) mice by FACS analyses (see Figure S2 for the gating strategy). The FACS data showed that $ROR\gamma t^+$ ILC3 (Figures 1A and 1D), as well as $NKp46^+$ (Figures 1B and 1E), LTi4, and LTi0 (Figures 1C and 1F) subsets, were all markedly decreased in $VDR^{-/-}$ mice at steady state compared with WT mice, independent of sexes.

To eliminate the potential confounding influence of T and B lymphocytes on ILC3 in the context of VDR ablation, we generated $Rag1^{-/-}VDR^{+/+}$ and $Rag1^{-/-}VDR^{-/-}$ mice that lacked mature T and B lymphocytes (Mombaerts et al., 1992). FACS analyses confirmed that the colonic $CD3^-ROR\gamma t^+$ ILC3 population, as well as LTi4 and LTi0 subsets, but not $NKp46^+$ cells, remained reduced in $Rag1^{-/-}VDR^{-/-}$ mice compared with $Rag1^{-/-}VDR^{+/+}$ controls (Figures S3A–S3F), indicating that the effect of VDR deletion on gut ILC3 abundance, particularly the LTi4 and LTi0 cells, is completely independent of T and B cells.

In contrast to gut $ROR\gamma t^+$ T cells (e.g., T_H17), the development of gut $ROR\gamma t^+$ ILC3 is pre-programmed and does not require gut commensal bacteria (Sawa et al., 2010). To address whether gut commensal bacteria affects gut ILC3 in the absence of VDR, we depleted gut microbiota from WT and $VDR^{-/-}$ mice by 4-week antibiotic treatment as described previously (Mukherji et al., 2013; Rakoff-Nahoum et al., 2004). Fecal bacterial 16S rRNA gene was almost undetectable by PCR following antibiotic treatment, confirming that the antibiotics had effectively depleted gut bacteria (Figure S4A). FACS data showed that colonic ILC3 profiles, including $CD3^-ROR\gamma t^+$ ILC3 and the $NKp46^+$, LTi4 and LTi0 subpopulations, remained suppressed in $VDR^{-/-}$ mice compared with WT controls in the context of the microbiota depletion (Figures S4B–S4G), suggesting that VDR regulation of gut ILC3 is independent of the commensal bacteria.

$VDR^{-/-}$ Mice Develop Impaired Immunity against *Citrobacter rodentium*

To assess the immunological implication of gut ILC3 reduction in $VDR^{-/-}$ mice, we analyzed their immune response to *Citrobacter rodentium* infection, a model widely used to assess ILC3-mediated immunity (Koroleva et al., 2015). Following oral gavage of *C. rodentium*, $VDR^{-/-}$ mice showed marked weight loss compared with WT mice (Figure 2A), and about 40% $VDR^{-/-}$ mice died during the infection course (about 30% died within 5 days post infection) (Figure 2B). We quantified fecal *C. rodentium* using MacConkey agar plates (Bouladoux et al., 2017), on which *C. rodentium* colonies formed distinctive morphology characterized by a pink center with white rim (Figure S5A). Furthermore, we also validated the identity of *C. rodentium* by PCR amplification of the virulence *eae* gene, which is DBS100 strain specific (Petty et al., 2010; Schauer and Falkow, 1993) (Figure S5B). Following infection, the fecal *C. rodentium* counts increased daily before reaching the peak by day 7, followed by bacterial clearance. The peak bacterial count of $VDR^{-/-}$ mice was >4 times higher compared with that of WT

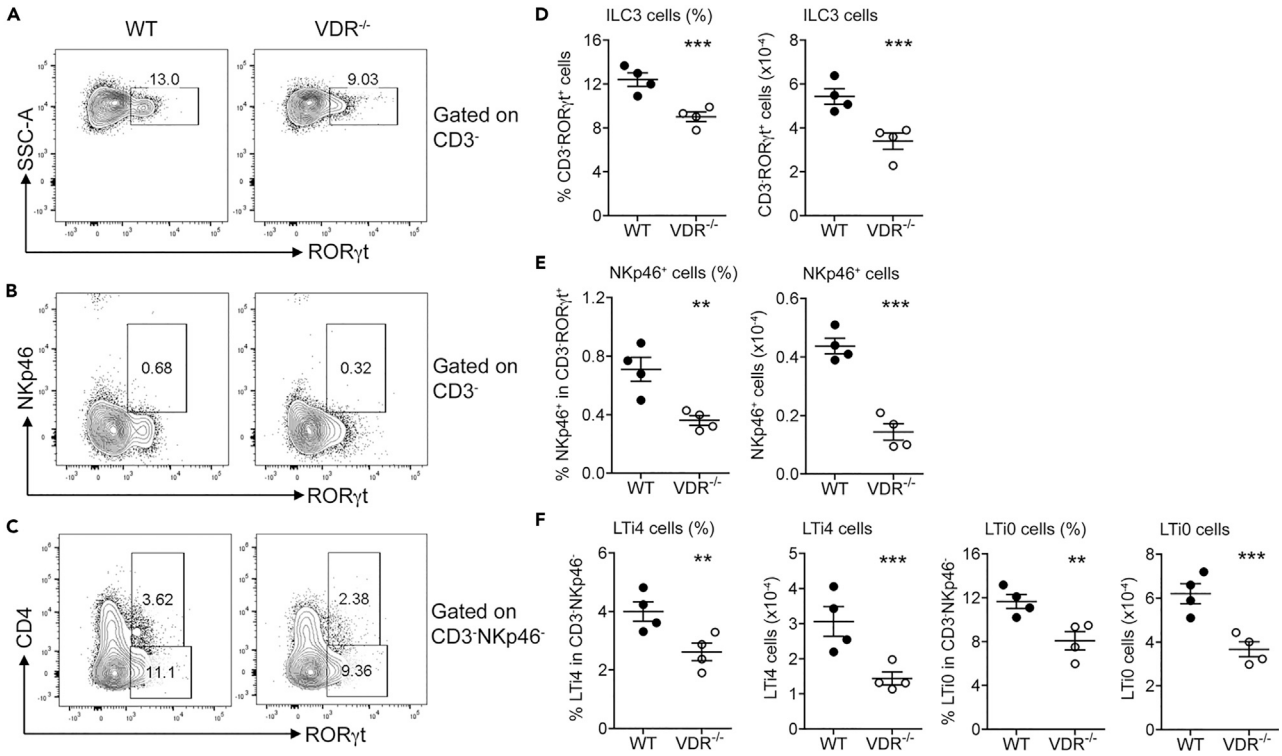

Figure 1. Global VDR Deletion Impairs Gut ILC3 Development in Mice

Colonic lamina propria (LP) cells were isolated from WT and VDR$^{-/-}$ mice, and the cells were analyzed by FACS for ILC3 populations.

(A–C) Representative FACS plots for analysis of RORγt^{+}ILC3 (A), NKp46^{+} cells (B), and LTi4 and LTi0 cells (C) in WT and VDR$^{-/-}$ mice at steady state.

(D–F) Quantitation based on FACS data of RORγt^{+}ILC3 (D), NKp46^{+} cells (E), and LTi4 and LTi0 cells (F) in WT and VDR$^{-/-}$ mice. The data were presented as percentage of the gated population and absolute cell number. **$p < 0.01$; ***$p < 0.001$. n = 4 each genotype. Data are represented as mean ± SEM.

mice. In fact, in VDR$^{-/-}$ mice the increase in fecal bacterial loads was one to two order of magnitude higher each day before reaching the peak, yet the bacterial clearance rate was substantially slower in comparison with WT counterparts (Figure 2C). FACS analyses detected a robust ILC3 response in WT mice, as total ILC3 population as well as IL-22^{+}ILC3, NKp46^{+}, LTi4, and LTi0 subsets were all markedly increased on day 5 after *C. rodentium* infection (Figures 2D–2J). In contrast, VDR$^{-/-}$ mice showed a clearly impaired ILC3 response; the induction of ILC3, IL-22^{+}ILC3, NKp46^{+}, LTi4, and LTi0 cells were all markedly attenuated (Figures 2D–2J). Particularly, IL-22^{+} ILC3 was almost not induced (Figures 2E and 2H). Thus, impaired ILC3 response, particularly attenuated IL-22 production, is likely the cause for the dramatic increase in bacterial growth in the gut of VDR$^{-/-}$ mice leading to their high mortality.

Deficiency in 1,25(OH)$_2$D$_3$ Impairs Gut ILC3 Development and ILC3-Mediated Immunity

Cyp27b1$^{-/-}$ mice are completely deficient in 1,25(OH)$_2$D$_3$ production, as they carry a genetic deletion in the 1α-hydroxylase gene (Panda et al., 2001), the rate-limiting enzyme required for 1,25(OH)$_2$D$_3$ biosynthesis. To assess whether the regulatory effect of VDR on ILC3 is ligand dependent, we compared the colonic ILC3 profiles between WT and Cyp27b1$^{-/-}$ mice at steady state and under *C. rodentium* infection. FACS analyses revealed marked decreases in CD3^{-}RORγt^{+} ILC3 populations at the steady state in Cyp27b1$^{-/-}$ mice compared with WT mice (Figures S6A and S6B, and Figures 3C–3I). When infected with *C. rodentium*, Cyp27b1$^{-/-}$ mice displayed much more severe body weight loss (Figure 3A) and higher fecal bacterial loads on days 2 and 5 (Figure 3B). FACS analyses showed that ILC3-mediated immunity was clearly impaired in Cyp27b1$^{-/-}$ mice. On day 5 after infection, ILC3 responses, including the increase in CD3^{-}RORγt^{+} ILC3, NKp46^{+}, LTi4, and LTi0 cells, were all markedly attenuated in Cyp27b1$^{-/-}$ mice compared with WT controls (Figures 3C–3I). Importantly, the induction of the IL-22^{+}ILC3 population was severely compromised in Cyp27b1$^{-/-}$ mice (Figures 3D and 3G). These data are similar to those of the ILC3 phenotype seen in VDR$^{-/-}$ mice, indicating that either VDR deletion or VDR ligand deficiency can lead to gut ILC3 deficiency and impaired ILC3-mediated immunity.

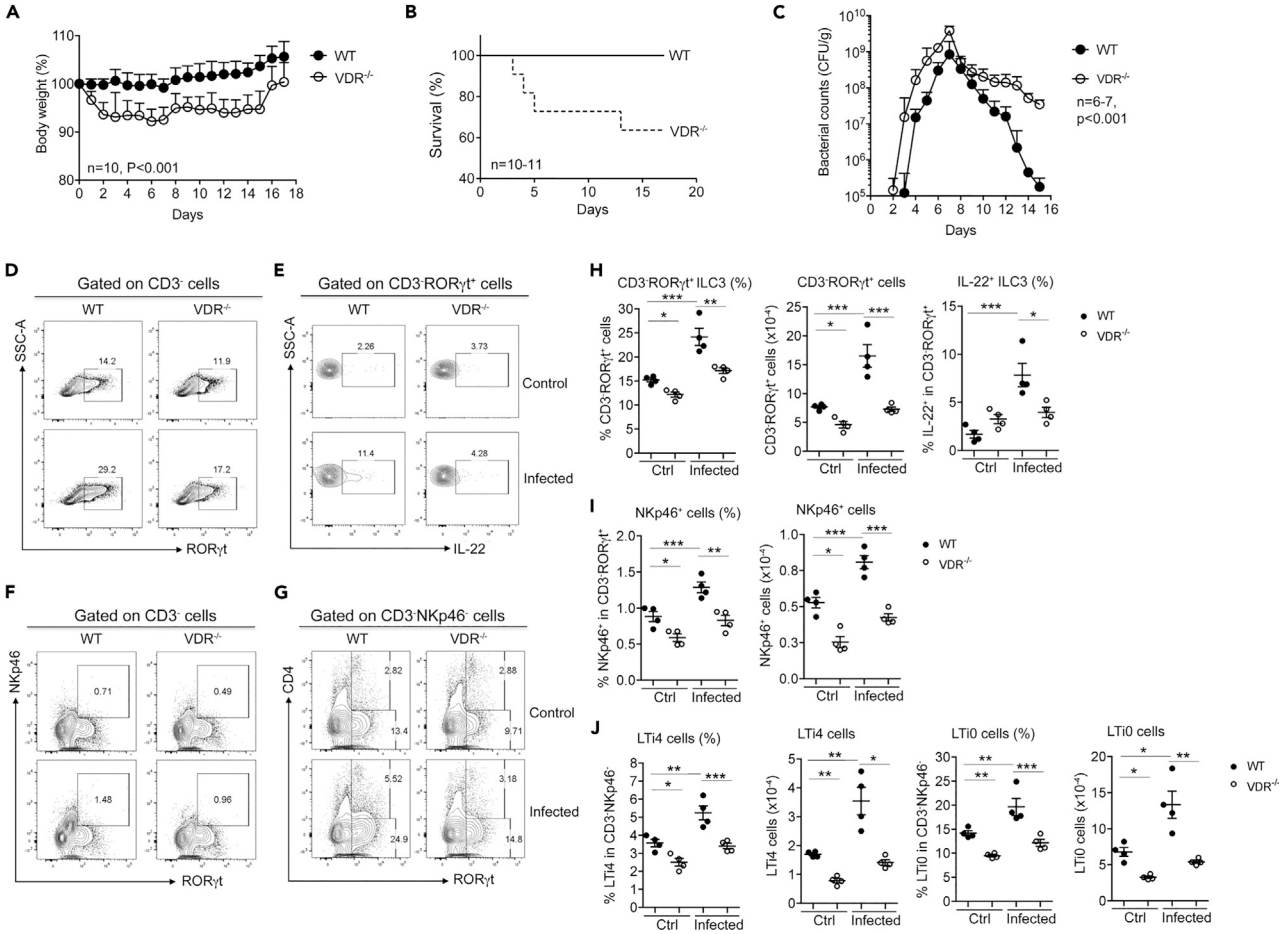

Figure 2. Global VDR Deletion Leads to Impaired Gut Immunity against *C. rodentium*

WT and VDR$^{-/-}$ mice were gavaged with *C. rodentium*. The mice were monitored daily for 16 days post infection. The mice were killed on day 5 following infection for FACS analyses of colonic LP cells.

(A–C) (A) Body weight changes (n = 10), (B) survival curve (n = 10–11), and (C) fecal daily bacterial counts (CFU) per gram of feces in WT and VDR$^{-/-}$ mice under *C. rodentium* infection (n = 6–7). $p < 0.001$ by log rank test.

(D–G) Representative FACS plots for the analysis of RORγt^{+}ILC3 (D), IL-22^{+}ILC3 (E), NKp46^{+} (F), and LTi4 and LTi0 cells (G) in WT and VDR$^{-/-}$ mice at steady state (Ctrl) and under *C. rodentium* infection.

(H–J) Quantitation RORγt^{+}ILC3 and IL-22^{+}ILC3 (H), NKp46^{+} cells (I), and LTi4 and LTi0 cells (J) in WT and VDR$^{-/-}$ mice at baseline and under *C. rodentium* infection. The data were presented as percentage of the gated population and absolute cell number. *$p < 0.05$; **$p < 0.01$; ***$p < 0.001$. n = 4 each group. Data are represented as mean ± SEM.

To confirm that 1,25(OH)$_2$D$_3$ is required for ILC3 development, we reconstituted Cyp27b1$^{-/-}$ mice with 1,25(OH)$_2$D$_3$ through daily intraperitoneal injection for one week. FACS analyses showed that 1,25(OH)$_2$D$_3$ reconstitution was able to partially correct gut ILC3 deficiency in Cyp27b1$^{-/-}$ mice. The total ILC3 population was substantially recovered following 1 week of 1,25(OH)$_2$D$_3$ injection. Specifically, LTi4 and LTi0 subsets, but not NKp46^{+} cells, were partially increased by 1,25(OH)$_2$D$_3$ treatment (Figure S7). Therefore, both 1,25(OH)$_2$D$_3$ and VDR are required for normal ILC3 development and function in the gut, especially for the LTi cells.

Critical Roles of ILC3-intrinsic VDR Signaling in the Regulation of ILC3

The effect of global VDR deletion in VDR$^{-/-}$ mice on ILC3 could be influenced by many confounding factors in the body. To specifically delineate the role of ILC3-intrinsic VDR signaling in ILC3 regulation, we generated VDR$^{flox/flox}$;RORγt-Cre mice that carried VDR deletion in ILC3. VDR$^{flox/flox}$;RORγt-Cre mice showed a marked and significant reduction in steady-state colonic CD3^{-}RORγt^{+}ILC3 population compared with VDR$^{flox/flox}$ mice (Figures 4C and 4G). The baseline IL-22^{+}ILC3 population was slightly

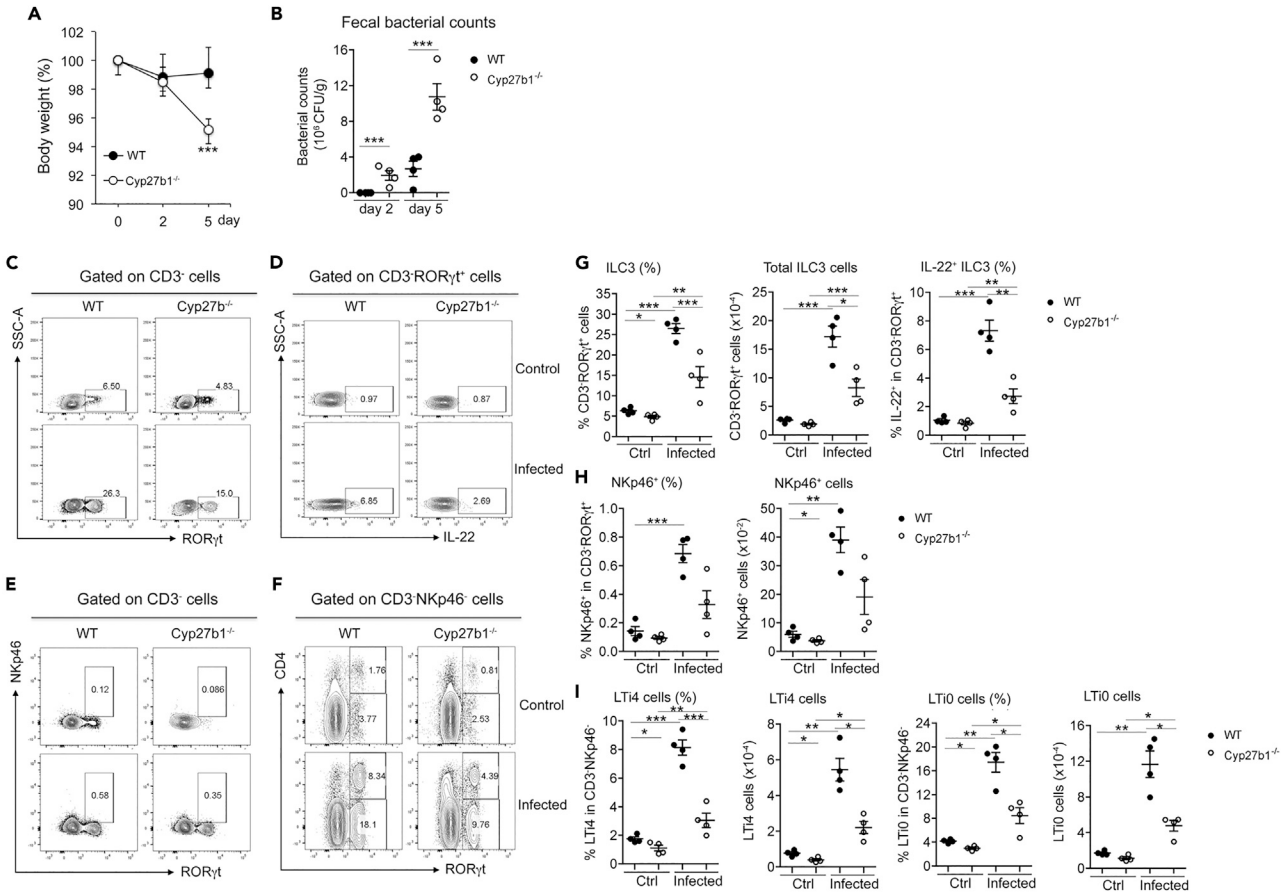

Figure 3. Deficiency in 1,25(OH)$_2$D$_3$ Synthesis Impairs ILC3 Development and Its Immunity against *C. rodentium*

WT and Cyp27b1$^{-/-}$ mice were gavaged with *C. rodentium*. The mice were killed on day 5 following infection for FACS analyses of colonic LP cells.

(A and B) (A) Body weight changes; (B) fecal bacterial counts per gram of feces in WT and Cyp27b1$^{-/-}$ mice on days 2 and 5 following *C. rodentium* infection. ***p < 0.001 vs. WT. n = 4–5 each group.

(C–F) Representative FACS plots for the analysis of RORγt$^+$ILC3 (C), IL-22$^+$ILC3 (D), NKp46$^+$ (E), and LTi4 and LTi0 cells (F) in WT and Cyp27b1$^{-/-}$ mice at steady state (Ctrl) and under *C. rodentium* infection.

(G–I) Quantitation RORγt$^+$ILC3 and IL-22$^+$ILC3 (G), NKp46$^+$ cells (H), and LTi4 and LTi0 cells (I) in WT and Cyp27b1$^{-/-}$ mice at baseline and under *C. rodentium* infection.

The data were presented as percentage of the gated population and absolute cell number. *p < 0.05; **p < 0.01; ***p < 0.001. n = 4 each group. Data are represented as mean ± SEM.

higher, which may reflect an intrinsic feedback mechanism to maintain IL-22 expression (Figures 4D and 4G). Specifically, the LTi4 and LTi0 subsets, but not NKp46$^+$ cells, were significantly decreased in VDR$^{flox/flox}$;RORγt-Cre mice at the steady state (Figures 4E, 4F, 4H, and 4I), confirming a critical role of ILC3-intrinsic VDR in the basal development of ILC3, particularly the LTi subsets. When VDR$^{flox/flox}$ and VDR$^{flox/flox}$;RORγt-Cre mice were infected with *C. rodentium*, VDR$^{flox/flox}$;RORγt-Cre mice showed more severe body weight loss and much higher fecal bacterial counts on day 4 compared with VDR$^{flox/flox}$ mice (Figures 4A and 4B). ILC3 responses, including the increases in CD3$^-$RORγt$^+$ ILC3 and LTi4 and LTi0 subsets (not NKp46$^+$) were markedly attenuated in VDR$^{flox/flox}$;RORγt-Cre mice (Figures 4C–4I). Particularly, the IL-22$^+$ILC3 population failed to be induced in VDR$^{flox/flox}$;RORγt-Cre mice (Figures 4D and 4G). Thus, ILC3-intrinsic VDR deletion impairs the ILC3 baseline development as well as ILC3-mediated immunity, indicating a critical role of ILC3-intrinsic vitamin D/VDR signaling in ILC3 biology.

RORγt is the master transcription factor in ILC3 and T_H17 lineages, but it may also express in other tissues; as such, RORγt-Cre could be leaky to other cells/tissues. To confirm that it was VDR deletion

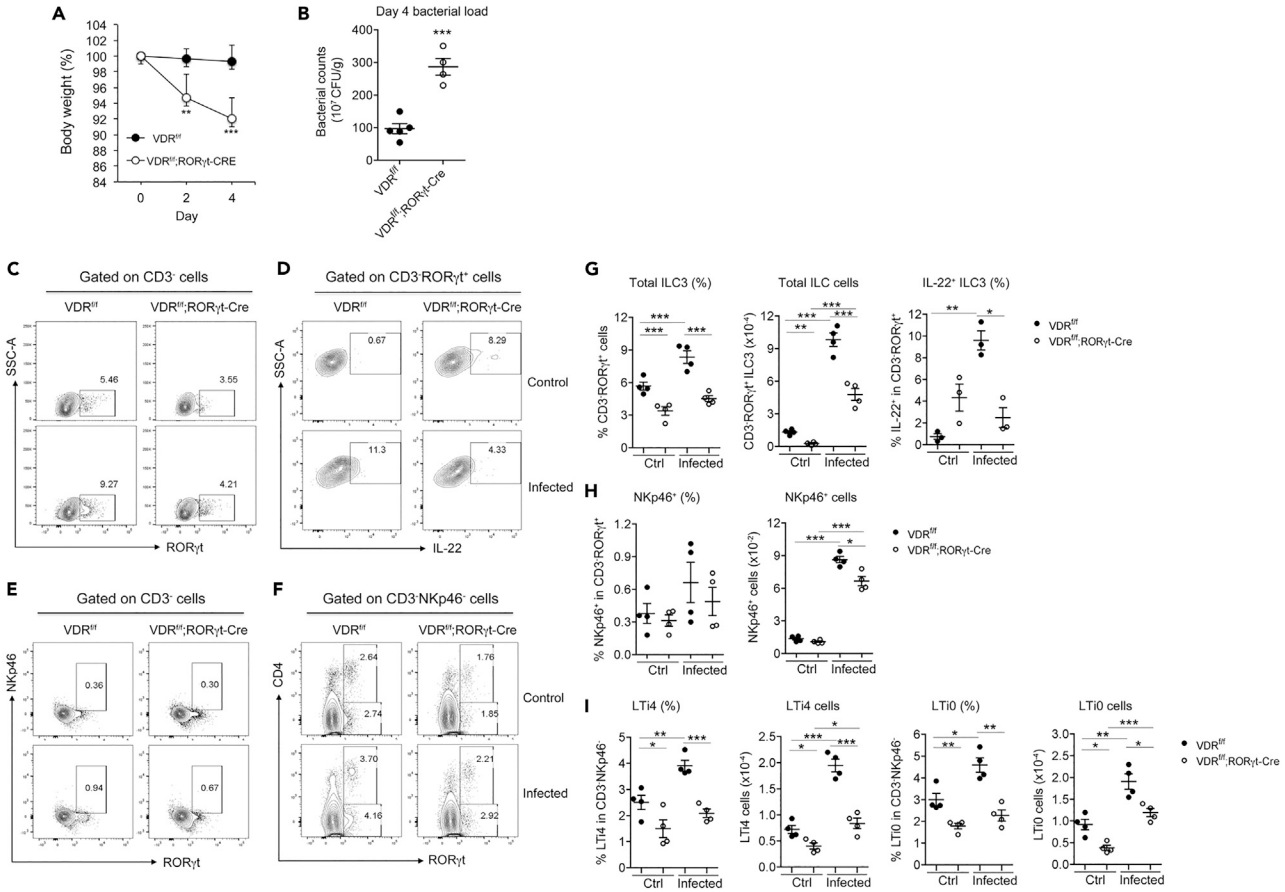

Figure 4. ILC3-specific Deletion of VDR Impairs ILC3 Development and Its Immunity against *C. rodentium* Infection

$VDR^{flox/flox}$ and $VDR^{flox/flox}$;RORγt-Cre mice were gavaged with *C. rodentium*. The mice were killed on day 4 following infection.

(A and B) (A) Body weight changes; (B) fecal bacterial counts per gram of feces in $VDR^{flox/flox}$ and $VDR^{flox/flox}$;RORγt-Cre mice on day 4 after *C. rodentium* infection. ***$p < 0.001$ vs. $VDR^{flox/flox}$. n = 4–5 each genotype.

(C–F) Representative FACS plots for the analysis of $ROR\gamma t^+$ILC3 (C), IL-22^+ILC3 (D), $NKp46^+$ (E), and LTi4 and LTi0 cells (F) in $VDR^{flox/flox}$ and $VDR^{flox/flox}$;RORγt-Cre mice at steady state (Ctrl) and under *C. rodentium* infection.

(G–I) Quantitation $ROR\gamma t^+$ILC3 and IL-22^+ILC3 (G), $NKp46^+$ cells (H), and LTi4 and LTi0 cells (I) in $VDR^{flox/flox}$ and $VDR^{flox/flox}$;RORγt-Cre mice at baseline and under *C. rodentium* infection.

The data were presented as percentage of the gated population and absolute cell number. *$p < 0.05$; **$p < 0.01$; ***$p < 0.001$. n = 4 each group. Data are represented as mean ± SEM.

in ILC3 that led to ILC3 defects, we transplanted $Rag1^{-/-}$ mice with bone marrow (BM) cells obtained from $VDR^{flox/flox}$ or $VDR^{flox/flox}$;RORγt-Cre mice using procedures as previously reported (Szeto et al., 2012). The success of the BM transplantation was validated in a parallel control experiment in which CD45.2 $VDR^{-/-}$ BM cells were transplanted to CD45.1 recipient mice (Figure S8). As shown in Figure S8, 8 weeks after transplantation, $CD45.2^+$ cells repopulated the blood and colonic lamina propria of the CD45.1 recipients. Importantly, the recipient's $ROR\gamma t^+$ cells (which include ILC3) were now $CD45.2^+$. Interestingly, 8 weeks after transplantation, $Rag1^{-/-}$ mice receiving $VDR^{flox/flox}$;RORγt-Cre BM cells still had significantly lower $CD3^-ROR\gamma t^+$ILC3 population as well as lower LTi4 and LTi0 subpopulations compared with $Rag1^{-/-}$ mice receiving $VDR^{flox/flox}$ BM cells (Figures 5A and 5B). These results confirmed that the ILC3-intrinsic VDR signaling indeed directly regulates ILC3 development, particularly the LTi subsets.

Vitamin D/VDR Signaling Regulates ILC3 Proliferation

To address how vitamin D/VDR signaling regulates ILC3 development, we assess the effect of VDR deletion on ILC3 apoptosis and proliferation, two processes that potentially determine the abundance of gut ILC3.

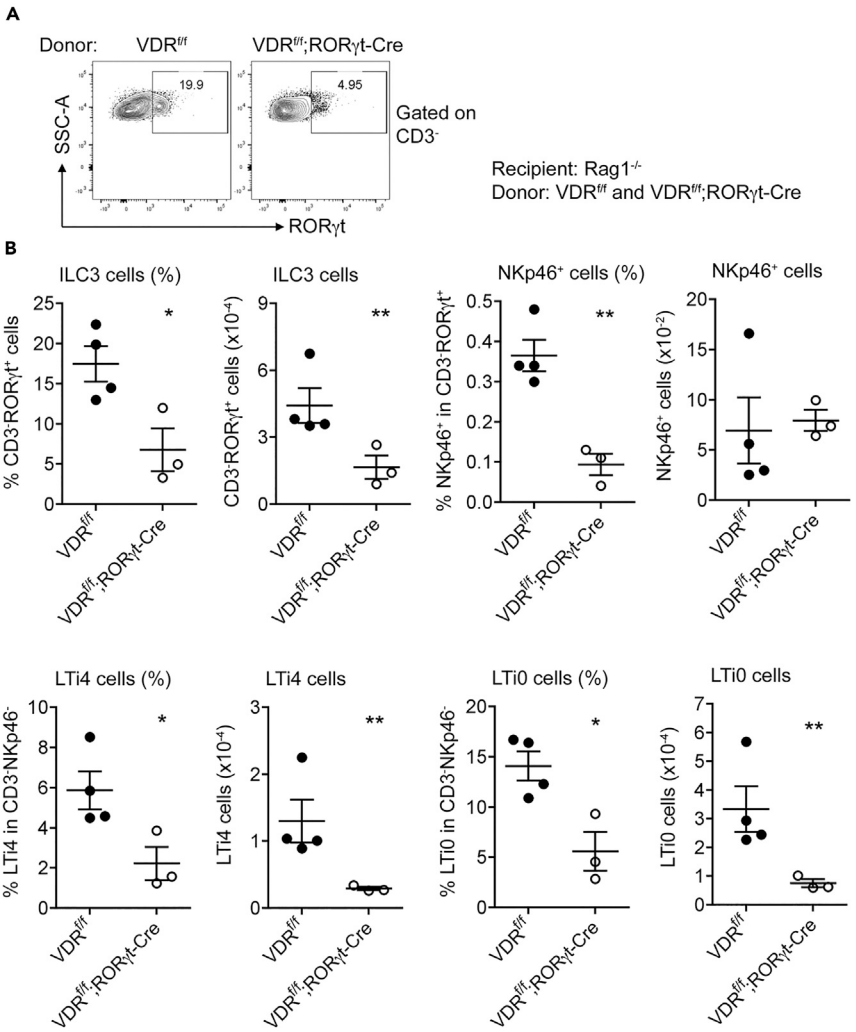

Figure 5. Bone Marrow (BM) Transplantation Confirms VDR Deletion in ILC3 Leading to Impaired ILC3 Development

BM cells obtained from $VDR^{flox/flox}$ or $VDR^{flox/flox}$/RORγt-Cre mice were transplanted to recipient $Rag1^{-/-}$ mice 6 h after receiving lethal γ-irradiation. The recipient mice were analyzed 8 weeks after transplantation.

(A and B) (A) Representative FACS plots for $ROR\gamma t^{+}$ILC3 analyses; (B) quantitation of colonic $ROR\gamma t^{+}$ILC3, $NKp46^{+}$, and LTi4 and LTi0 cells in recipient mice transplanted with $VDR^{flox/flox}$ or $VDR^{flox/flox}$;RORγt-Cre BM cells. The data were presented as percentage of the gated population and absolute cell number. *$p < 0.05$, **$p < 0.01$. n = 3–4 each group. Data are represented as mean ± SEM.

To assess ILC3 apoptosis, we generated $VDR^{-/-}Rorc^{gfp/+}$ mice whose ILC3 is marked by GFP. FACS analyses found no differences between $VDR^{+/+}Rorc^{gfp/+}$ and $VDR^{-/-}Rorc^{gfp/+}$ mice in Annexin V^{+}/7-AAD^{+} and Annexin V^{+}/7-AAD^{-} cells among all the gut ILC3 populations (Figure S9), suggesting that ILC3 defects caused by VDR deletion is not due to excessive ILC3 apoptosis. We then quantified ILC3 proliferation by Ki67 staining. Remarkably, $Ki67^{+}$ cells in the $CD3^{-}ROR\gamma t^{+}$ILC3 population as well as in LTi4 and LTi0 subsets were clearly decreased at steady state in $VDR^{-/-}$ mice (Figures 6A and 6B), $VDR^{flox/flox}$;RORγt-Cre mice (Figures 6C and 6D), and $Cyp27b1^{-/-}$ mice (Figures 6E and 6F) compared with $VDR^{+/+}$ mice, $VDR^{flox/flox}$ mice, and $Cyp27b1^{+/+}$ mice, respectively. Under *C. rodentium* infection, the $Ki67^{+}$ ILC3 cells, including $CD3^{-}ROR\gamma t^{+}$ cells and LTi4 and LTi0 subsets, were dramatically induced in $VDR^{+/+}$ mice and $VDR^{flox/flox}$ mice, but the induction was greatly attenuated in $VDR^{-/-}$ mice and $VDR^{flox/flox}$;RORγt-Cre mice (Figures 6A–6D). In these three mouse models, however, there were almost no changes in $Ki67^{+}NKp46^{+}$ cells (Figures 6A–6F). These observations suggest that the vitamin D/VDR signaling plays a key role in the regulation of gut ILC3 expansion, mainly the LTi cells.

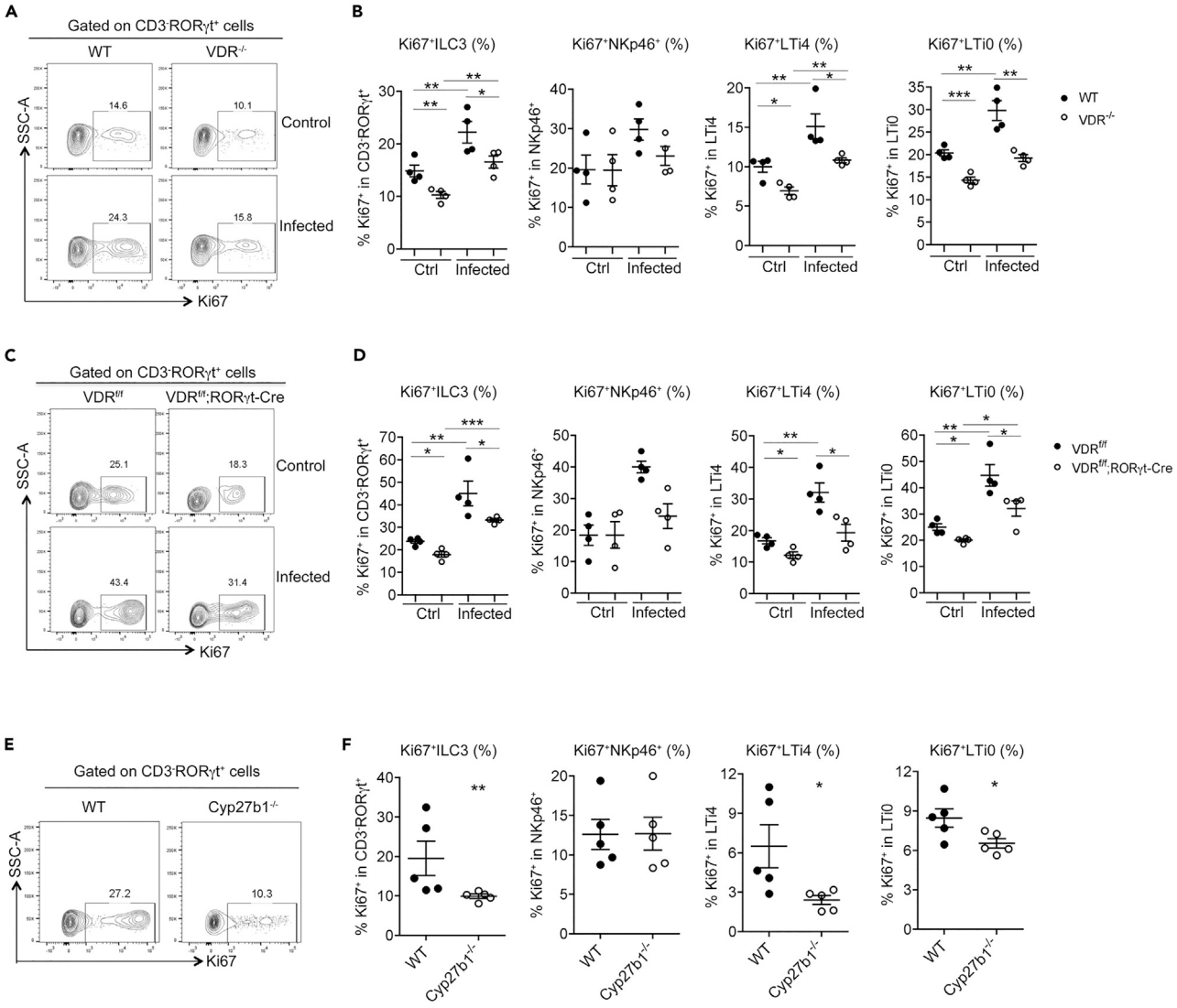

Figure 6. Deletion of VDR or Cyp27b1 Reduces ILC3 Proliferation

Colonic LP cells were isolated from WT or $VDR^{-/-}$ mice at steady state (Ctrl) or under *C. rodentium* infection for 5 days (A and B), from $VDR^{flox/flox}$ or $VDR^{flox/flox}$;RORγt-Cre mice at steady state or under *C. rodentium* infection for 5 days (Cand D), or from WT and $Cyp27b1^{-/-}$ mice at steady state (E and F). $Ki67^+$ ILC3 and ILC3 subsets were quantified by FACS. (A, C, and E) Representative FACS plots for $Ki67^+$ $ROR\gamma t^+$ILC3; (B, D, and F) quantitation of $Ki67^+ROR\gamma t^+$ILC3 and $Ki67^+NKp46^+$, $Ki67^+$LTi4, and $Ki67^+$LTi0 subsets. *p < 0.05; **p < 0.01; ***p < 0.001. n = 4–5 each group. Data are represented as mean ± SEM.

To confirm this notion, we further examined the effect of VDR activation by its ligand on ILC3 proliferation. As shown in Figure 7, reconstitution of $Cyp27b1^{-/-}$ mice with $1,25(OH)_2D_3$ by 1-week daily injection was able to mostly restore the $Ki67^+$ ILC3 populations ($CD3^-ROR\gamma t^+$, LTi4, LTi0) in the colonic mucosa (Figure 7A). Moreover, daily treatment of WT mice with a low calcemic vitamin D analogue, paricalcitol, for 1 week was able to substantially stimulate colonic $Ki67^+$ ILC3 populations ($CD3^-ROR\gamma t^+$, LTi4 and LTi0) (Figure 7B). Consistently, there were little effects from these treatments on $Ki67^+$ $NKp46^+$ cells (Figures 7A and 7B).

To address whether vitamin D/VDR signaling directly regulates ILC3 proliferation, we FACS-sorted $Lin^-Thy1.2^{hi}KLRG1^-IL\text{-}7R\alpha^+$ cells from colonic LP cells from $Rag1^{-/-}$ mice as described previously (Spencer et al., 2014) (see Figure S10 for the sorting strategy) and then cultured these cells for 3 days in a medium containing IL-7 and stem cell factor (SCF) in the presence or absence of $1,25(OH)_2D_3$ before quantifying the $Ki67^+$ ILC3 population by FACS. We found that $1,25(OH)_2D_3$ treatment was able to increase the

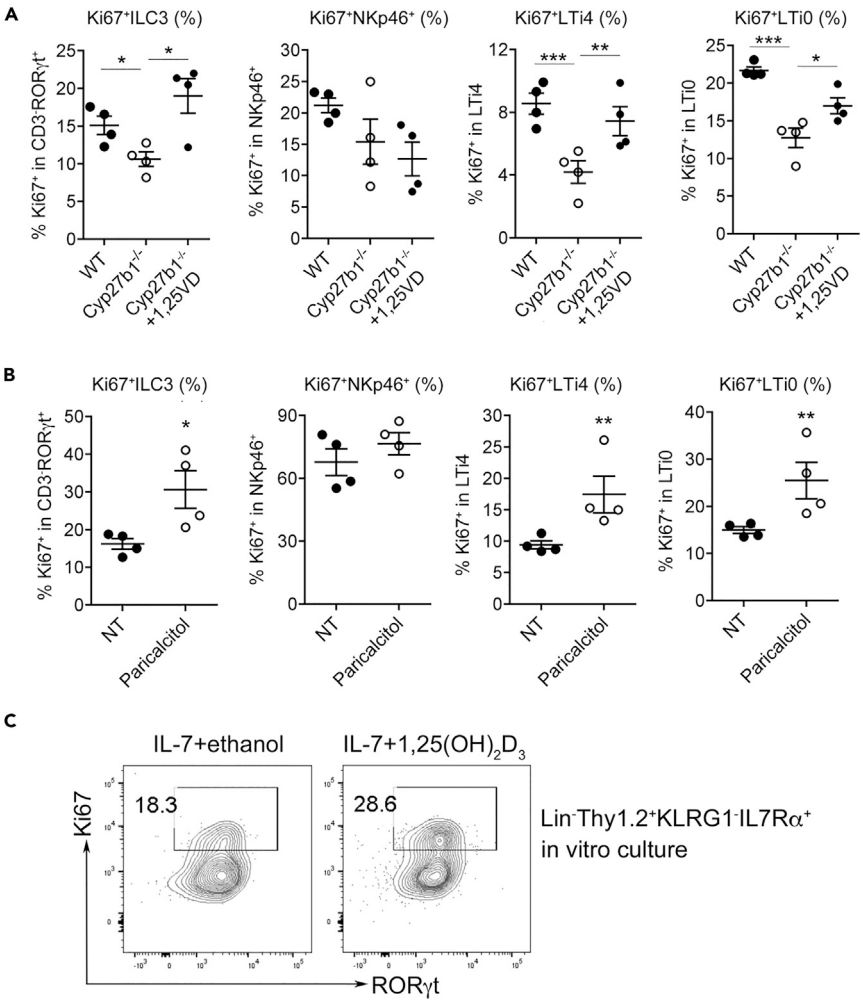

Figure 7. Ligand Activation of VDR Stimulates ILC3 Proliferation

(A) FACS quantitation of colonic Ki67$^+$RORγt$^+$ILC3 and Ki67$^+$NKp46$^+$, Ki67$^+$LTi4, and Ki67$^+$LTi0 subpopulations in WT, Cyp27b1$^{-/-}$ or Cyp27b1$^{-/-}$ mice treated with 1,25(OH)$_2$D$_3$ for 1 week; (B) FACS quantitation of colonic Ki67$^+$RORγt$^+$ILC3 and Ki67$^+$NKp46$^+$, Ki67$^+$LTi4, and Ki67$^+$LTi0 subsets in WT untreated or treated with paricalcitol for 1 week; (C) Lin$^-$Thy1.2^{hi}KLRG1$^-$IL-7Rα$^+$ cells were sorted by FACS and cultured in the presence or absence of 1,25(OH)$_2$D$_3$ for 3 days, and Ki67$^+$RORγt$^+$ILC3 population was analyzed by FACS. Shown are representative FACS plots. *$p < 0.05$, **$p < 0.01$; ***$p < 0.001$. n = 4 each group. Data are represented as mean ± SEM.

Ki67$^+$RORγt$^+$ cell population by >56% *in vitro* (Figure 7C). This is compelling evidence demonstrating that the vitamin D/VDR signaling indeed directly stimulates ILC3 proliferation.

DISCUSSION

In this report we presented several lines of evidence to demonstrate that the vitamin D/VDR signaling pathway critically regulates ILC3 development and function in the gut. We showed that VDR deletion caused a marked reduction in gut ILC3 populations and compromises ILC3-mediated innate immunity against bacterial infection. This regulatory action of VDR on ILC3 is independent of T and B lymphocytes and gut commensal bacteria. We also showed that the deficiency of 1,25(OH)$_2$D$_3$, the VDR ligand, basically phenocopied VDR deficiency in terms of affecting gut ILC3 development and function, indicating that the regulatory action of VDR on ILC3 is ligand dependent. Given that the majority of VDR actions is known to be dependent on 1,25(OH)$_2$D$_3$, the similar ILC3 phenotypes seen in VDR$^{-/-}$ and Cyp27b1$^{-/-}$ mice actually provide a strong confirmation for the reliability of our findings. By specifically deleting VDR

from ILC3 we further demonstrated that the ILC3-intrisinc VDR signaling is required for normal development and function of ILC3. Our data suggest that promoting ILC3 proliferation and differentiation is an important mechanism whereby the vitamin D/VDR signaling regulates ILC3. Together these findings extend our understanding of the immunoregulatory activities of the vitamin D/VDR signaling in innate immunity.

Although it is well established that the vitamin D endocrine system regulates immune responses (Hart et al., 2011; Mora et al., 2008), few studies have explored the effect of vitamin D and VDR on innate lymphoid cells. A previous study by Chen et al. reported that global VDR deletion caused dysbiosis, which conferred resistance to *C. rodentium* infection to VDR knockout mice because of increased ILC3 and antimicrobial peptides; however, elimination of gut microbiota with antibiotics rendered VDR knockout mice more susceptible to *C. rodentium* than control mice. These findings are inconsistent with our results. However, this same study also showed that elimination of T and B lymphocytes from VDR knockout mice ($Rag1^{-/-}VDR^{-/-}$ mice) increased their susceptibility to *C. rodentium* infection when compared with controls (Chen et al., 2015), which is consistent with our findings reported here, confirming the notion that the VDR regulation of ILC3 is independent of functional T and B lymphocytes. This prior report, although interesting, provided no clear answers as to whether and how VDR influences ILC3. Additionally, there are two other reports by Ryz et al. that studied the relationship between vitamin D and *C. rodentium* infection but not ILC3. One paper showed that vitamin D deficiency increased mouse's susceptibility to *C. rodentium* mostly because of increased production of pro-inflammatory cytokines (Ryz et al., 2015), and the other showed that 1,25-dihydroxyvitamin D treatment also increased mouse's susceptibility to *C. rodentium* mostly because of the suppression of T_H17 response (Ryz et al., 2012). Together these unsettled and seemingly contradictory studies provide a strong rationale to explore the roles of the vitamin D/VDR signaling pathway in ILC3 regulation and in *C. rodentium* infection. Therefore, in the current study we employed a series of genetic mouse models to tackle these important issues.

As the biological action of the vitamin D endocrine system depends on both the vitamin D hormone and its receptor, we studied genetic models that lack either the receptor (VDR knockout) or the ability to synthesize the vitamin D hormone (Cyp27b1 knockout). We also examined VDR knockout mice that lack mature T and B lymphocytes ($Rag1^{-/-}/VDR^{-/-}$ mice) or commensal microflora to eliminate the potentially confounding effects of the adaptive immune system and microbiota on the results. Because VDR knockout mice develop many abnormalities (Bouillon et al., 2008) that may interfere with data interpretation, we further studied $VDR^{flox/flox}$;RORγt-Cre mice that lack VDR signaling in ILC3 as well as lethally irradiated mice that are repopulated with $VDR^{flox/flox}$;RORγt-Cre bone marrow cells. These cell-specific deletion and bone marrow transplantation models generated compelling evidence for a direct and critical role of VDR in ILC3 biology. In addition to ILC3, RORγt is also expressed in T_H17 and T_{reg} cells; thus $VDR^{flox/flox}$;-RORγt-Cre mice may carry VDR deletion in ILC3 as well as in T^H17 and T_{reg} cells. However, because we had already demonstrated that VDR deletion in T cells did not influence the effect of VDR on ILC3, particularly the LTi cells (see Figure S3, $Rag1^{-/-}/VDR^{-/-}$ mice), the $VDR^{flox/flox}$;RORγt-Cre mice thus allowed us to study and elucidate the intrinsic role of ILC3 VDR in ILC3 regulation. Indeed, the intrinsic stimulatory effect of vitamin D/VDR on ILC3 was confirmed in the *in vitro* ILC3 culture (Figure 7C). Furthermore, in this study we analyzed not only the $CD3^-ROR\gamma t^+$ cells but also the $NKp46^+$ and LTi0/4 subsets. The data from these models all firmly support the notion that the vitamin D/VDR signaling is required for the development and anti-bacterial function of gut ILC3. In the absence of $1,25(OH)_2D_3$ or VDR, gut ILC3 populations markedly decreased and failed to proliferate leading to impaired immunity against *C. rodentium*. Particularly, the IL-22-producing ILC3 population failed to expand in response to *C. rodentium* infection, which likely accounts for the severe bacterial growth and high mortality seen in the mutant mice, because IL-22 released from LTi4 cells in the first 6 days following *C. rodentium* infection is the major IL-22 source to counter the infection (Sonnenberg et al., 2011). In fact, the results from all our mouse models, as well as from *in vitro* ILC3 culture, are very consistent to show that the vitamin D/VDR signaling promotes the proliferation of LTi cells, but the effect on $NKp46^+$ cells is inconsistent. That is, our data strongly suggest that the mechanism responsible for vitamin D/VDR regulation of ILC3-mediated innate immunity lies in its stimulation of proliferation of LTi0 and LTi4 cells, but not $NKp46^+$ cells. Since $NKp46^+$ and LTi cells are derived from different precursors (Artis and Spits, 2015), it is not surprising that the vitamin D/VDR activity has different effects on these cells. In fact, whether vitamin D regulates $NKp46^+$ cells or not should not have a meaningful impact on vitamin D-regulated ILC3 immunity, as $NKp46^+$ cells or NKp46-derived IL-22 only plays a minor role in innate immunity against *C. rodentium* (Cella et al., 2009). Therefore, given the importance of LTi cells,

future studies should be focused on how vitamin D/VDR regulates LTi cell proliferation and LTi-mediated immunity.

IL-22 is a key cytokine produced by ILC3 that plays key roles in host defense against infection as well as in tissue remodeling and maintenance of mucosal barrier integrity (Artis and Spits, 2015; Bernink et al., 2013). The latter is overlapped with the mucosal barrier-protecting activity of the vitamin D/VDR signaling (Du et al., 2015; He et al., 2018; Liu et al., 2013). It is conceivable that vitamin D/VDR may also protect the integrity of the mucosal barrier through regulating IL-22 production from ILC3. Here our data suggest that vitamin D/VDR regulates IL-22 synthesis through controlling ILC3 proliferation, but it is also possible that VDR directly regulates IL-22 gene expression, as seen in other nuclear receptors such as RORγt$^+$ and AHR (Qiu et al., 2012; Sawa et al., 2010). A most recent study reported that vitamin D/VDR downregulates IL-23 receptor-mediated pathway in human NKp44$^+$ ILC3 (mouse NKp46$^+$ equivalent), suppressing IL-22 expression (Konya et al., 2018). This *in vitro* observation in human ILC3 appears in contrast to our *in vivo* finding, but it is irrelevant because our studies have shown that vitamin D/VDR has little effects on NKp46$^+$ cells in mice. The reason behind the discrepancy between humans and mice in terms of vitamin D regulation of NKp44$^+$/NKp46$^+$ cells is unclear.

There have been increasing interests in the anti-infectious activity of vitamin D. A good example is a study that demonstrated how vitamin D stimulates anti-microbial activity in macrophages against *Mycobacterium tuberculosis* (Liu et al., 2006). Here we show that vitamin D also stimulates potent innate immunity against *C. rodentium* infection via gut ILC3. The results from these investigations suggest that the vitamin D endocrine system has intrinsic anti-infectious and anti-bacterial activity to serve the host defense system. In this regard, maintaining appropriate vitamin D levels in the body is important for an effective host defense against infection.

Limitations of the Study

In this study we presented strong evidence that the vitamin D/VDR signaling is required for proper proliferation and function of ILC3, particularly the LTi0 and LTi4 cells at baseline and under pathogenic bacterial infection; however, exactly how the vitamin D/VDR signaling regulates ILC3 proliferation remains unclear. Future studies are needed to elucidate the underlying molecular mechanism. Moreover, germ-free models are needed to confirm the effect of gut microbiota on vitamin D regulation of ILC3.

METHODS

All methods can be found in the accompanying Transparent Methods supplemental file.

SUPPLEMENTAL INFORMATION

Supplemental Information can be found online at https://doi.org/10.1016/j.isci.2019.06.026.

ACKNOWLEDGMENTS

We thank David Goltzman (McGill University) for providing the Cyp27b1 knockout mouse line and Wanyin Deng and B. Brett Finlay (University of British Columbia) for providing *Citrobacter rodentium* strains and technical assistance. This work was supported in part by National Institutes of Health grants CA180087 and NIDDK P30DK42086.

AUTHOR CONTRIBUTIONS

Conceptualization: Y.C.L.; Methodology and Investigation: L.H. and M.Z.; Formal analysis: L.H. and Y.C.L.; Writing – Original Draft: L.H. and Y.C.L.; Writing – Review & Editing: Y.C.L.; Fund Acquisition: Y.C.L.; Supervision: Y.C.L.

DECLARATION OF INTERESTS

The authors declare no competing interests.

Received: October 29, 2018
Revised: April 30, 2019
Accepted: June 14, 2019
Published: July 26, 2019

REFERENCES

Artis, D., and Spits, H. (2015). The biology of innate lymphoid cells. Nature *517*, 293–301.

Bernink, J., Mjosberg, J., and Spits, H. (2013). Th1- and Th2-like subsets of innate lymphoid cells. Immunol. Rev. *252*, 133–138.

Bouillon, R., Carmeliet, G., Verlinden, L., van Etten, E., Verstuyf, A., Luderer, H.F., Lieben, L., Mathieu, C., and Demay, M. (2008). Vitamin D and human health: lessons from vitamin D receptor null mice. Endocr. Rev. *29*, 726–776.

Bouladoux, N., Harrison, O.J., and Belkaid, Y. (2017). The mouse model of infection with *Citrobacter rodentium*. Curr. Protoc. Immunol. *119*, 19 15 11–19 15 25.

Cella, M., Fuchs, A., Vermi, W., Facchetti, F., Otero, K., Lennerz, J.K., Doherty, J.M., Mills, J.C., and Colonna, M. (2009). A human natural killer cell subset provides an innate source of IL-22 for mucosal immunity. Nature *457*, 722–725.

Chen, J., Waddell, A., Lin, Y.D., and Cantorna, M.T. (2015). Dysbiosis caused by vitamin D receptor deficiency confers colonization resistance to *Citrobacter rodentium* through modulation of innate lymphoid cells. Mucosal. Immunol. *8*, 618–626.

Du, J., Chen, Y., Shi, Y., Liu, T., Cao, Y., Tang, Y., Ge, X., Nie, H., Zheng, C., and Li, Y.C. (2015). 1,25-Dihydroxyvitamin D protects intestinal epithelial barrier by regulating the myosin light chain kinase signaling pathway. Inflamm. Bowel Dis. *21*, 2495–2506.

Guo, X., Qiu, J., Tu, T., Yang, X., Deng, L., Anders, R.A., Zhou, L., and Fu, Y.X. (2014). Induction of innate lymphoid cell-derived interleukin-22 by the transcription factor STAT3 mediates protection against intestinal infection. Immunity *40*, 25–39.

Hart, P.H., Gorman, S., and Finlay-Jones, J.J. (2011). Modulation of the immune system by UV radiation: more than just the effects of vitamin D? Nat. Rev. Immunol. *11*, 584–596.

Haussler, M.R., Whitfield, G.K., Kaneko, I., Haussler, C.A., Hsieh, D., Hsieh, J.C., and Jurutka, P.W. (2013). Molecular mechanisms of vitamin D action. Calcif. Tissue Int. *92*, 77–98.

He, L., Liu, T., Shi, Y., Tian, F., Hu, H., Deb, D.K., Chen, Y., Bissonnette, M., and Li, Y.C. (2018). Gut epithelial vitamin D receptor regulates microbiota-dependent mucosal inflammation by suppressing intestinal epithelial cell apoptosis. Endocrinology *159*, 967–979.

Holick, M.F. (1996). Vitamin D: photobiology, metabolism, mechanism of action, and clinical application. In Primer on the Metabolic Bone Diseases and Disorders of Mineral Metabolism, Third Edition, M.J. Favus, ed. (Lippincott-Raven), pp. 74–81.

Holick, M.F. (2007). Vitamin D deficiency. N. Engl. J. Med. *357*, 266–281.

Holick, M.F. (2018). Photobiology of vitamin D. In Vitamin D, Fourth Edition, D. Feldman, ed. (Academic Press), pp. 45–55.

Joshi, S., Pantalena, L.C., Liu, X.K., Gaffen, S.L., Liu, H., Rohowsky-Kochan, C., Ichiyama, K., Yoshimura, A., Steinman, L., Christakos, S., et al. (2011). 1,25-dihydroxyvitamin D(3) ameliorates Th17 autoimmunity via transcriptional modulation of interleukin-17A. Mol. Cell Biol. *31*, 3653–3669.

Konya, V., Czarnewski, P., Forkel, M., Rao, A., Kokkinou, E., Villablanca, E.J., Almer, S., Lindforss, U., Friberg, D., Hoog, C., et al. (2018). Vitamin D downregulates the IL-23 receptor pathway in human mucosal group 3 innate lymphoid cells. J. Allergy Clin. Immunol. *141*, 279–292.

Koroleva, E.P., Halperin, S., Gubernatorova, E.O., Macho-Fernandez, E., Spencer, C.M., and Tumanov, A.V. (2015). *Citrobacter rodentium*-induced colitis: a robust model to study mucosal immune responses in the gut. J. Immunol. Methods *421*, 61–72.

Lee, S.M., Riley, E.M., Meyer, M.B., Benkusky, N.A., Plum, L.A., DeLuca, H.F., and Pike, J.W. (2015). 1,25-Dihydroxyvitamin D3 controls a cohort of vitamin D receptor target genes in the proximal intestine that is enriched for calcium-regulating components. J. Biol. Chem. *290*, 18199–18215.

Lemire, J.M., Adams, J.S., Kermani-Arab, V., Bakke, A.C., Sakai, R., and Jordan, S.C. (1985). 1,25-Dihydroxyvitamin D3 suppresses human T helper/inducer lymphocyte activity in vitro. J. Immunol. *134*, 3032–3035.

Liu, P.T., Stenger, S., Li, H., Wenzel, L., Tan, B.H., Krutzik, S.R., Ochoa, M.T., Schauber, J., Wu, K., Meinken, C., et al. (2006). Toll-like receptor triggering of a vitamin D-mediated human antimicrobial response. Science *311*, 1770–1773.

Liu, W., Chen, Y., Golan, M.A., Annunziata, M.L., Du, J., Dougherty, U., Kong, J., Musch, M., Huang, Y., Pekow, J., et al. (2013). Intestinal epithelial vitamin D receptor signaling inhibits experimental colitis. J. Clin. Invest. *123*, 3983–3996.

Mombaerts, P., Iacomini, J., Johnson, R.S., Herrup, K., Tonegawa, S., and Papaioannou, V.E. (1992). RAG-1-deficient mice have no mature B and T lymphocytes. Cell *68*, 869–877.

Mora, J.R., Iwata, M., and von Andrian, U.H. (2008). Vitamin effects on the immune system: vitamins A and D take centre stage. Nat. Rev. Immunol. *8*, 685–698.

Mukherji, A., Kobiita, A., Ye, T., and Chambon, P. (2013). Homeostasis in intestinal epithelium is orchestrated by the circadian clock and microbiota cues transduced by TLRs. Cell *153*, 812–827.

Panda, D.K., Miao, D., Tremblay, M.L., Sirois, J., Farookhi, R., Hendy, G.N., and Goltzman, D. (2001). Targeted ablation of the 25-hydroxyvitamin D 1alpha -hydroxylase enzyme: evidence for skeletal, reproductive, and immune dysfunction. Proc. Natl. Acad. Sci. U S A *98*, 7498–7503.

Penna, G., and Adorini, L. (2000). 1 Alpha,25-dihydroxyvitamin D3 inhibits differentiation, maturation, activation, and survival of dendritic cells leading to impaired alloreactive T cell activation. J. Immunol. *164*, 2405–2411.

Penna, G., Roncari, A., Amuchastegui, S., Daniel, K.C., Berti, E., Colonna, M., and Adorini, L. (2005). Expression of the inhibitory receptor ILT3 on dendritic cells is dispensable for induction of CD4+Foxp3+ regulatory T cells by 1,25-dihydroxyvitamin D3. Blood *106*, 3490–3497.

Petty, N.K., Bulgin, R., Crepin, V.F., Cerdeno-Tarraga, A.M., Schroeder, G.N., Quail, M.A., Lennard, N., Corton, C., Barron, A., Clark, L., et al. (2010). The *Citrobacter rodentium* genome sequence reveals convergent evolution with human pathogenic *Escherichia coli*. J. Bacteriol. *192*, 525–538.

Qiu, J., Heller, J.J., Guo, X., Chen, Z.M., Fish, K., Fu, Y.X., and Zhou, L. (2012). The aryl hydrocarbon receptor regulates gut immunity through modulation of innate lymphoid cells. Immunity *36*, 92–104.

Rakoff-Nahoum, S., Paglino, J., Eslami-Varzaneh, F., Edberg, S., and Medzhitov, R. (2004). Recognition of commensal microflora by toll-like receptors is required for intestinal homeostasis. Cell *118*, 229–241.

Rigby, W.F., Stacy, T., and Fanger, M.W. (1984). Inhibition of T lymphocyte mitogenesis by 1,25-dihydroxyvitamin D3 (calcitriol). J. Clin. Invest. *74*, 1451–1455.

Ryz, N.R., Lochner, A., Bhullar, K., Ma, C., Huang, T., Bhinder, G., Bosman, E., Wu, X., Innis, S.M., Jacobson, K., et al. (2015). Dietary vitamin D3 deficiency alters intestinal mucosal defense and increases susceptibility to *Citrobacter rodentium*-induced colitis. Am. J. Physiol. Gastrointest. Liver Physiol. *309*, G730–G742.

Ryz, N.R., Patterson, S.J., Zhang, Y., Ma, C., Huang, T., Bhinder, G., Wu, X., Chan, J., Glesby, A., Sham, H.P., et al. (2012). Active vitamin D (1,25-dihydroxyvitamin D3) increases host susceptibility to *Citrobacter rodentium* by suppressing mucosal Th17 responses. Am. J. Physiol. Gastrointest. Liver Physiol. *303*, G1299–G1311.

Sawa, S., Cherrier, M., Lochner, M., Satoh-Takayama, N., Fehling, H.J., Langa, F., Di Santo, J.P., and Eberl, G. (2010). Lineage relationship analysis of RORgammat+ innate lymphoid cells. Science *330*, 665–669.

Schauer, D.B., and Falkow, S. (1993). The eae gene of *Citrobacter freundii* biotype 4280 is necessary for colonization in transmissible murine colonic hyperplasia. Infect. Immun. *61*, 4654–4661.

Shirakawa, A.K., Nagakubo, D., Hieshima, K., Nakayama, T., Jin, Z., and Yoshie, O. (2008). 1,25-Dihydroxyvitamin D3 induces CCR10 expression in terminally differentiating human B cells. J. Immunol. *180*, 2786–2795.

Sonnenberg, G.F., and Artis, D. (2012). Innate lymphoid cell interactions with microbiota: implications for intestinal health and disease. Immunity *37*, 601–610.

Sonnenberg, G.F., Monticelli, L.A., Elloso, M.M., Fouser, L.A., and Artis, D. (2011). CD4(+)

lymphoid tissue-inducer cells promote innate immunity in the gut. Immunity *34*, 122–134.

Spencer, S.P., Wilhelm, C., Yang, Q., Hall, J.A., Bouladoux, N., Boyd, A., Nutman, T.B., Urban, J.F., Jr., Wang, J., Ramalingam, T.R., et al. (2014). Adaptation of innate lymphoid cells to a micronutrient deficiency promotes type 2 barrier immunity. Science *343*, 432–437.

Sugimoto, K., Ogawa, A., Mizoguchi, E., Shimomura, Y., Andoh, A., Bhan, A.K., Blumberg, R.S., Xavier, R.J., and Mizoguchi, A. (2008). IL-22 ameliorates intestinal inflammation in a mouse model of ulcerative colitis. J. Clin. Invest. *118*, 534–544.

Szeto, F.L., Reardon, C.A., Yoon, D., Wang, Y., Wong, K.E., Chen, Y., Kong, J., Liu, S.Q., Thadhani, R., Getz, G.S., et al. (2012). Vitamin D receptor signaling inhibits atherosclerosis in mice. Mol. Endocrinol. *26*, 1091–1101.

von Essen, M.R., Kongsbak, M., Schjerling, P., Olgaard, K., Odum, N., and Geisler, C. (2010). Vitamin D controls T cell antigen receptor signaling and activation of human T cells. Nat. Immunol. *11*, 344–349.

Wang, Y., Zhu, J., and DeLuca, H.F. (2012). Where is the vitamin D receptor? Arch. Biochem. Biophys. *523*, 123–133.

Wolk, K., Kunz, S., Witte, E., Friedrich, M., Asadullah, K., and Sabat, R. (2004). IL-22 increases the innate immunity of tissues. Immunity *21*, 241–254.

Zheng, Y., Valdez, P.A., Danilenko, D.M., Hu, Y., Sa, S.M., Gong, Q., Abbas, A.R., Modrusan, Z., Ghilardi, N., de Sauvage, F.J., et al. (2008). Interleukin-22 mediates early host defense against attaching and effacing bacterial pathogens. Nat. Med. *14*, 282–289.

ISCI, Volume *17*

Supplemental Information

Vitamin D/Vitamin D Receptor Signaling Is Required for Normal Development and Function of Group 3 Innate Lymphoid Cells in the Gut

Lei He, Min Zhou, and Yan Chun Li

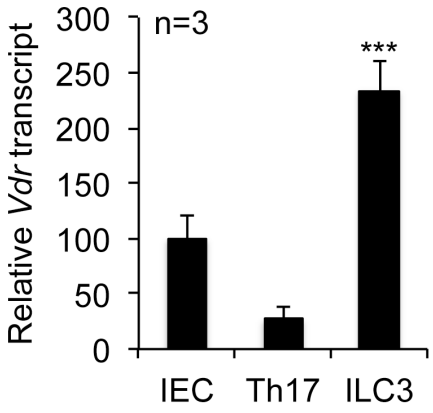

Figure S1. High level VDR expression in ILC3, Related to Figure 1.
Real time RT-PCR quantification of *Vdr* transcript in purified intestinal epithelial cells, and sorted T_H17 cells and ILC3. Data are represented as mean ± SEM.

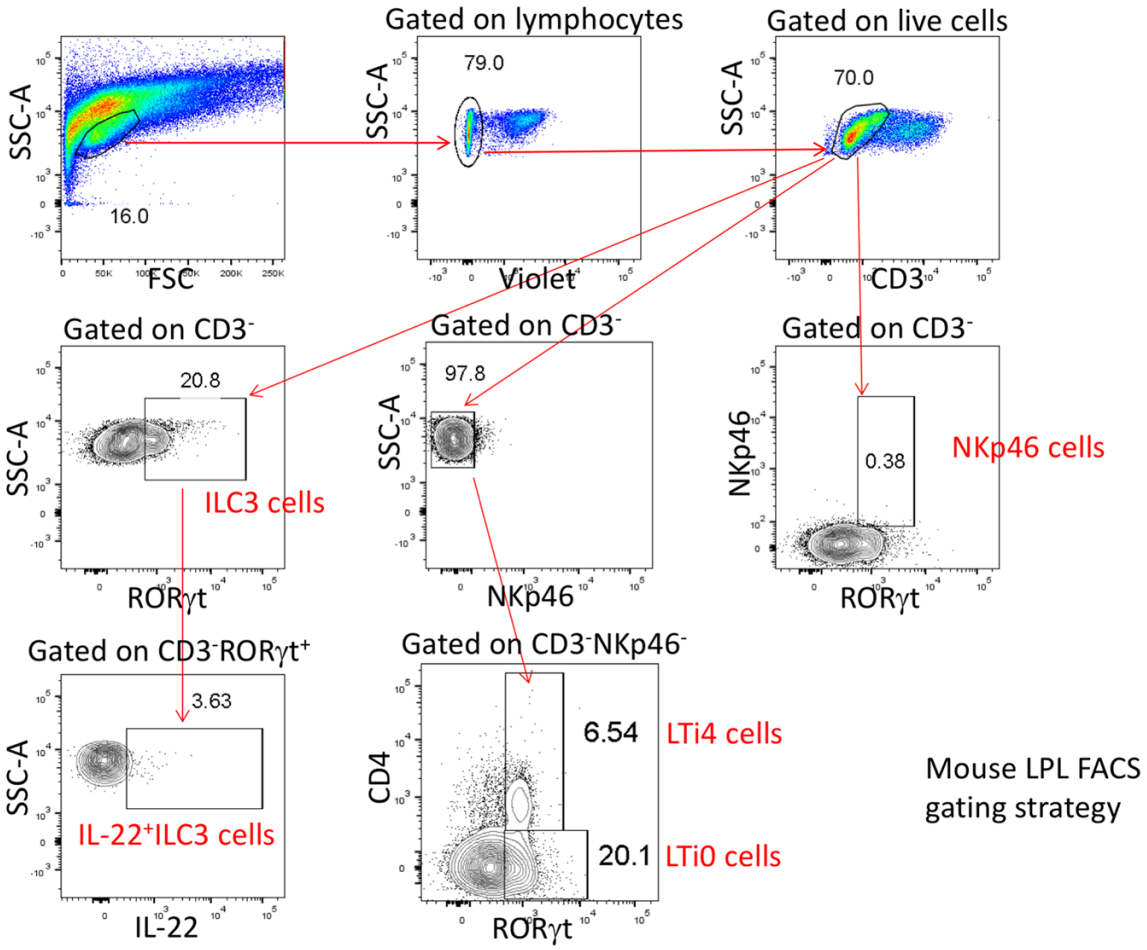

Figure S2. Flow cytometry gating strategies for FACS analyses of gut ILC3 and its sub-populations from lamina propria cells, Related to Figure 1.

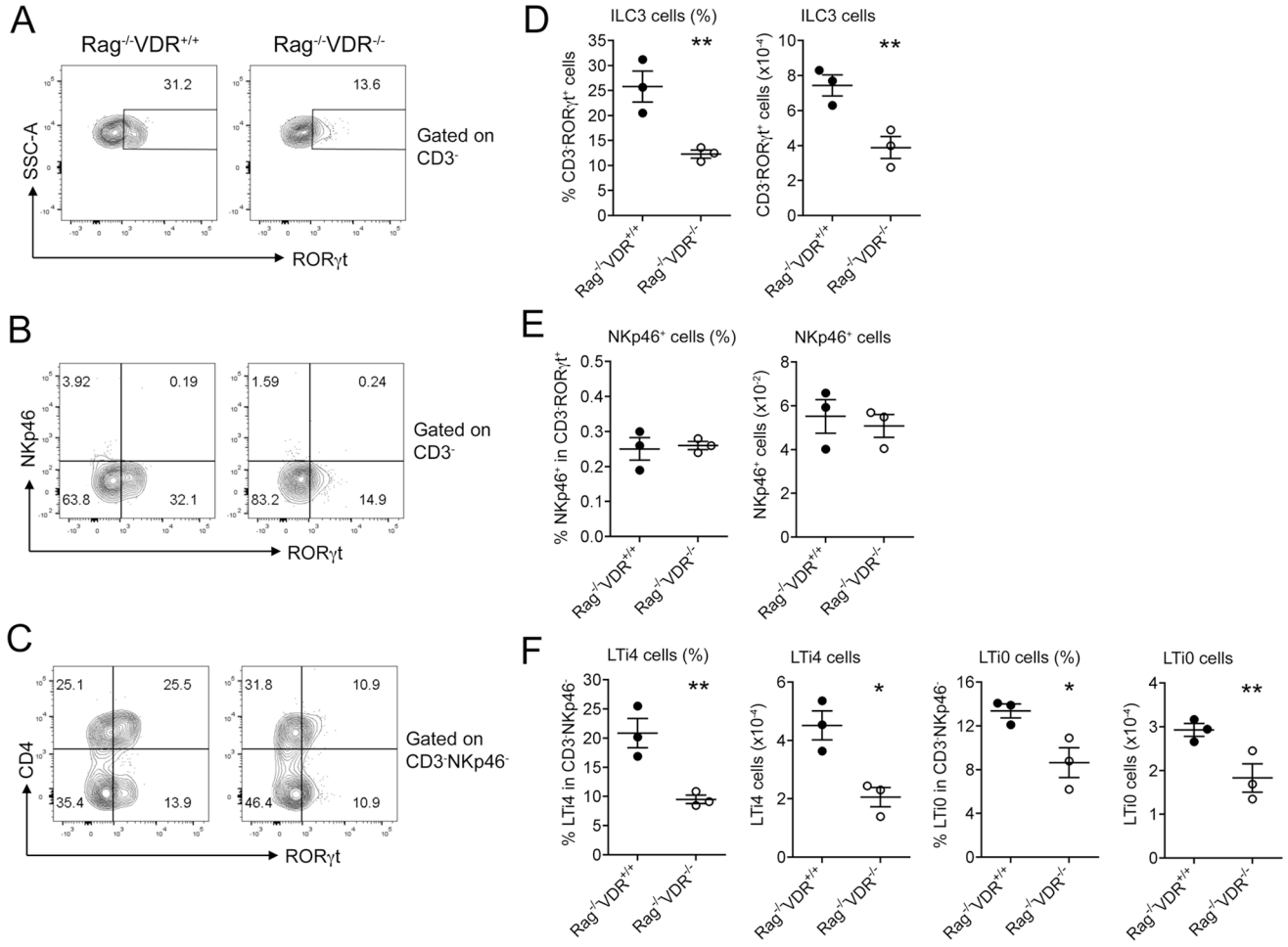

Figure S3. Effects of VDR deletion on gut ILC3 development is independent of T and B cells, Related to Figure 1.

Colonic lamina propria cells were isolated from Rag1$^{-/-}$VDR$^{+/+}$ and Rag1$^{-/-}$VDR$^{-/-}$ mice, and the cells were analyzed by FACS for ILC3 populations.

(A-C) Representative FACS plots for analysis of RORγt^{+}ILC3 (A), NKp46^{+} cells (B) and LTi4 and LTi0 cells (C) in Rag1$^{-/-}$VDR$^{+/+}$ and Rag1$^{-/-}$VDR$^{-/-}$ mice at steady state.

(D-F) Quantitation based on FACS data of RORγt^{+}ILC3 (D), NKp46^{+} cells (E) and LTi4 and LTi0 cells (F) in Rag1$^{-/-}$VDR$^{+/+}$ and Rag1$^{-/-}$VDR$^{-/-}$ mice.

The data were presented as percentage of the gated population and absolute cell number. *P<0.05; **P<0.01; ***P<0.001. n=3 each genotype. Data are represented as mean ± SEM.

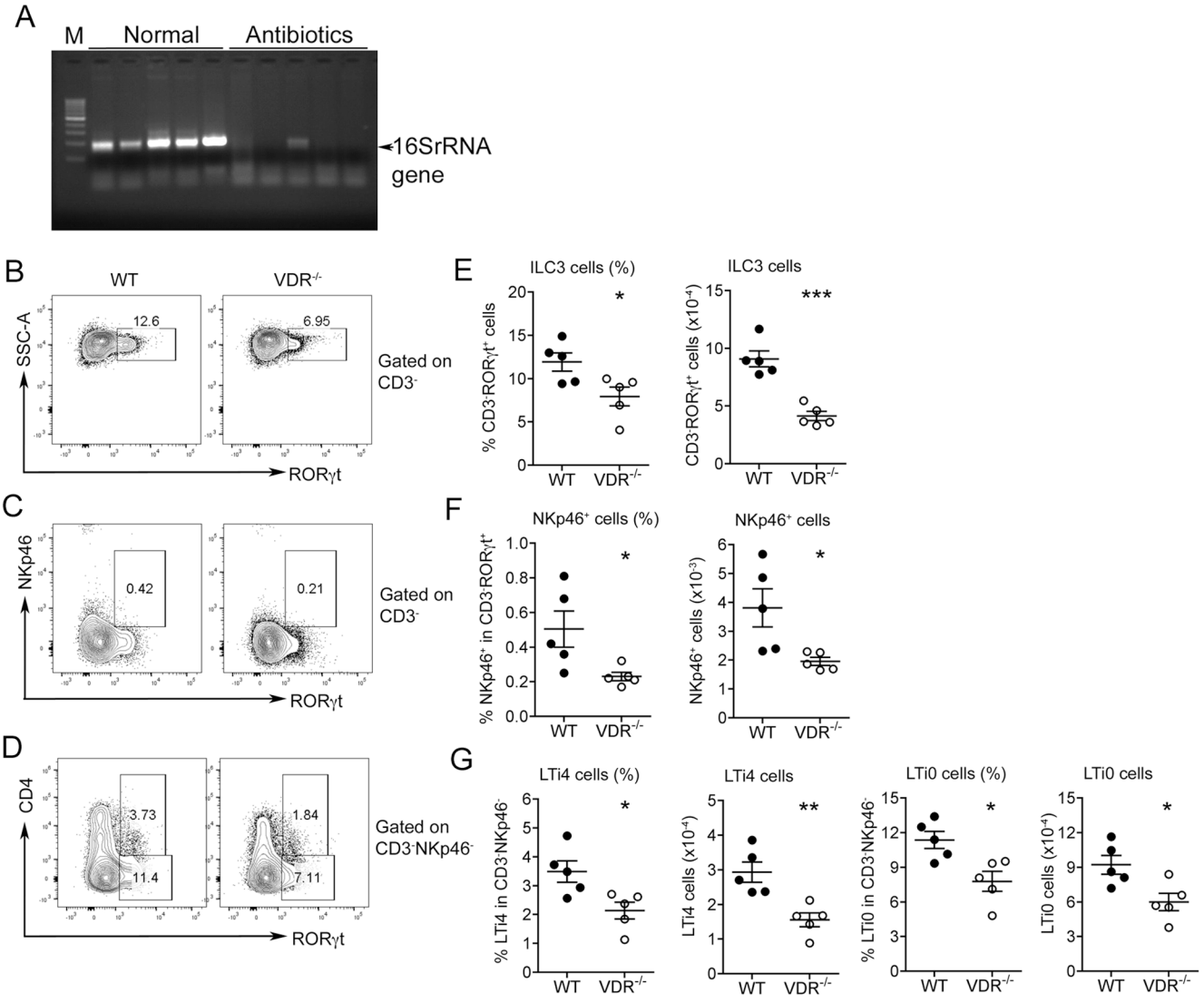

Figure S4. Effects of VDR deletion on gut ILC3 development is independent of gut commensal bacteria, Related to Figure 1.

Colonic lamina propria cells were isolated from WT and VDR$^{-/-}$ mice treated with the antibiotic cocktail for 4 weeks, and the cells were analyzed by FACS for ILC3 populations.

(A) PCR amplification of 16S rRNA gene from DNA purified from fecal pellets. Each lane contains DNA from two fecal pellets amplified by 25 PCR cycles. Each lane represents one mouse.

(B-D) Representative FACS plots for analysis of RORγt^{+}ILC3 (B), NKp46^{+} cells (C) and LTi4 and LTi0 cells (D).

(E-G) Quantitation based on FACS data of RORγt^{+}ILC3 (E), NKp46^{+} cells (F) and LTi4 and LTi0 cells (G).

The data were presented as percentage of the gated population and absolute cell number. *P<0.05; **P<0.01; ***P<0.001. n=5 each genotype. Data are represented as mean ± SEM.

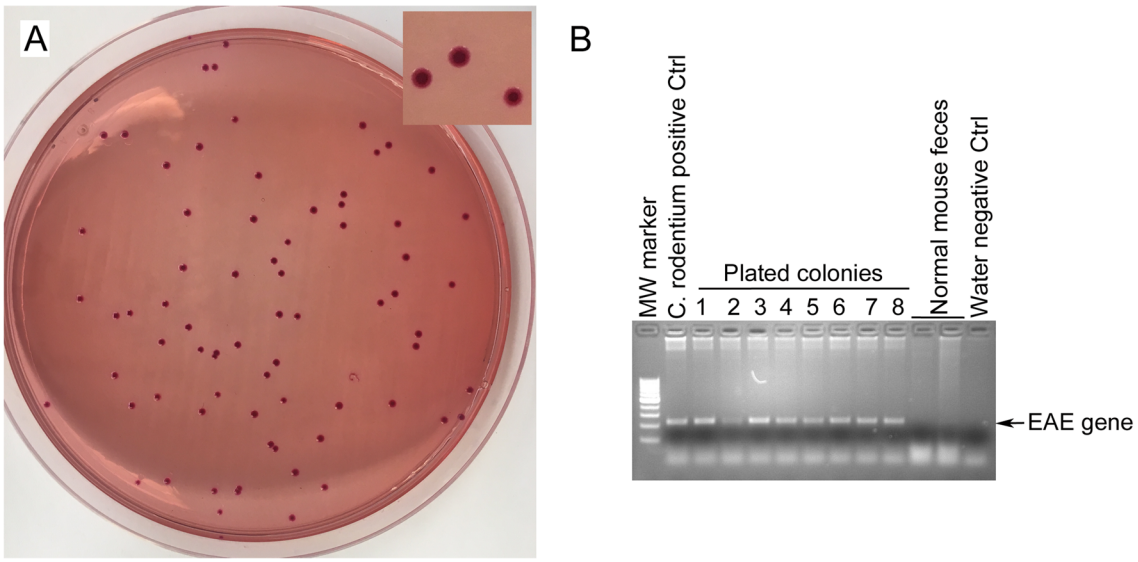

Figure S5. Quantitation of fecal *C. rodentium*, Related to Figure 2.
(A) Representative MacConkey agar plate showing *C. rodentium* colonies, whose distinctive morphology is characterized by a pink center with white rim. *Inset* shows an enlarged image of the colonies.
(B) PCR amplification of the *eae* gene from 8 randomly picked colonies. The *eae* gene was undetectable from normal, uninfected mouse feces.

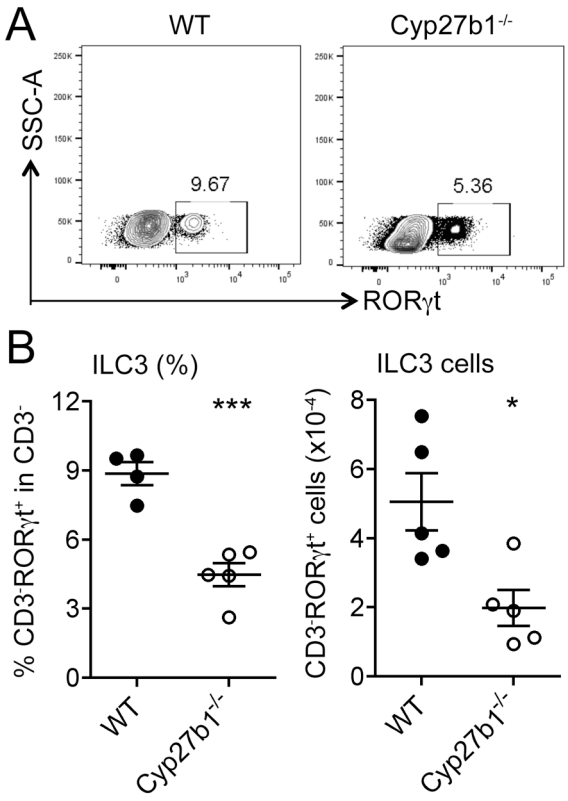

Figure S6. 1,25(OH)$_2$D$_3$ deficiency impairs gut ILC3 development, Related to Figure 3.
Colonic lamina propria cells were isolated from WT and Cyp27b1$^{-/-}$ mice, and the cells were analyzed by FACS for ILC3 populations.
(A) Representative FACS plots for analysis of RORγt$^+$ILC3;
(B) Quantitation of RORγt$^+$ILC3 in percentage and absolute cell number. *P<0.05; ***P<0.001. n=4-5 each genotype.

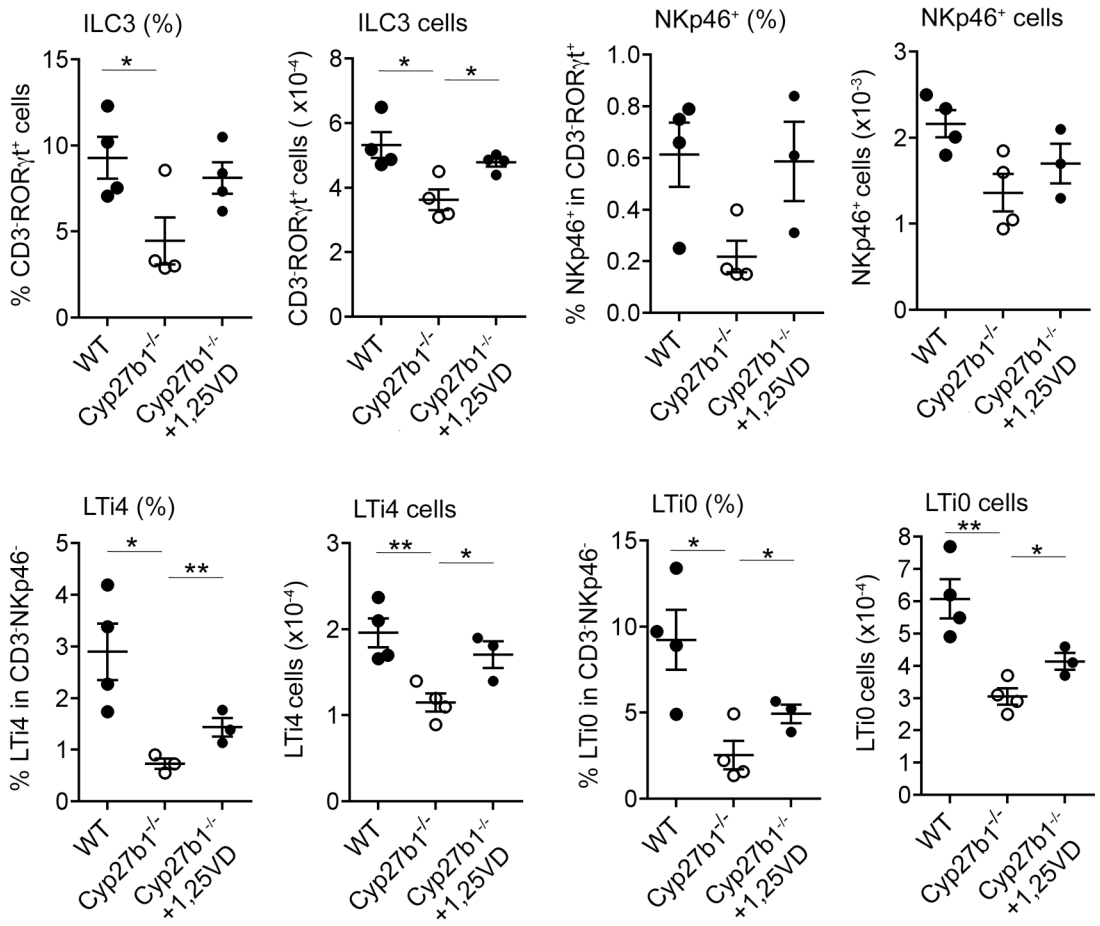

Figure S7. Reconstitution of Cyp27b1$^{-/-}$ mice with 1,25(OH)$_2$D$_3$ restores gut ILC3 populations, Related to Figure 3.

Colonic LP cells were isolated from WT, Cyp27b1$^{-/-}$ or Cyp27b1$^{-/-}$ mice treated with 1,25(OH)$_2$D$_3$ for one week, and gut ILC3 populations were quantified by FACS analyses. Shown are quantitation of RORγt$^+$ILC3, NKp46$^+$ cells, and LTi4 and LTi0 cells in percentage and absolute cell number. *P<0.05; **P<0.01; ***P<0.001. n=3-4 each group. Data are represented as mean ± SEM.

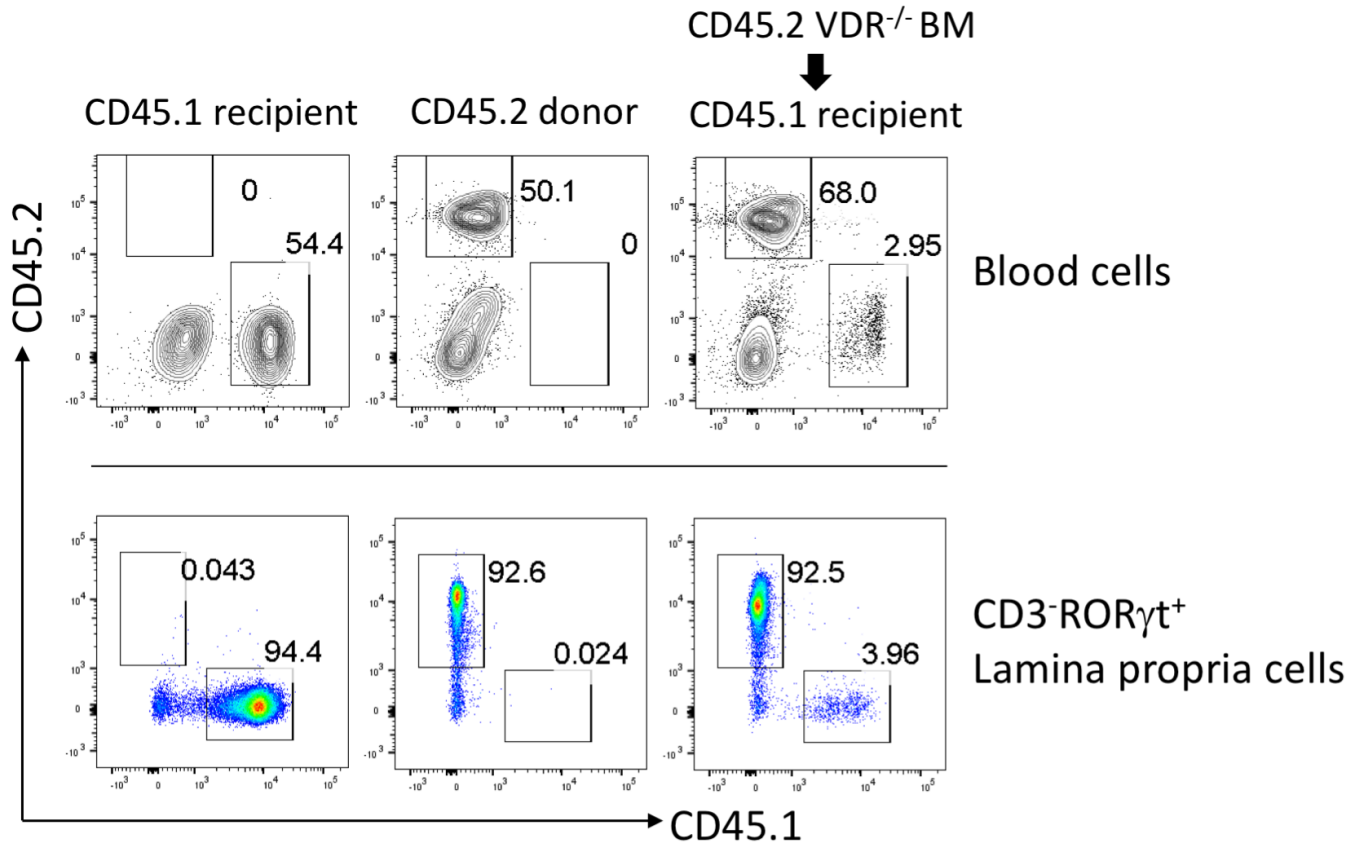

Figure S8. Validation of bone marrow transplantation, Related to Figure 5.
Bone marrow cells isolated from CD45.2 VDR-/- mice were transplanted to lethally irradiated CD45.1 recipient mice. Eight weeks later, blood and colonic lamina propria cells were analyzed by FACS. Note after transplantation the blood cells and colonic $CD3^{-}ROR\gamma t^{+}$ cells of the CD45.1 recipients had become CD45.2 positive.

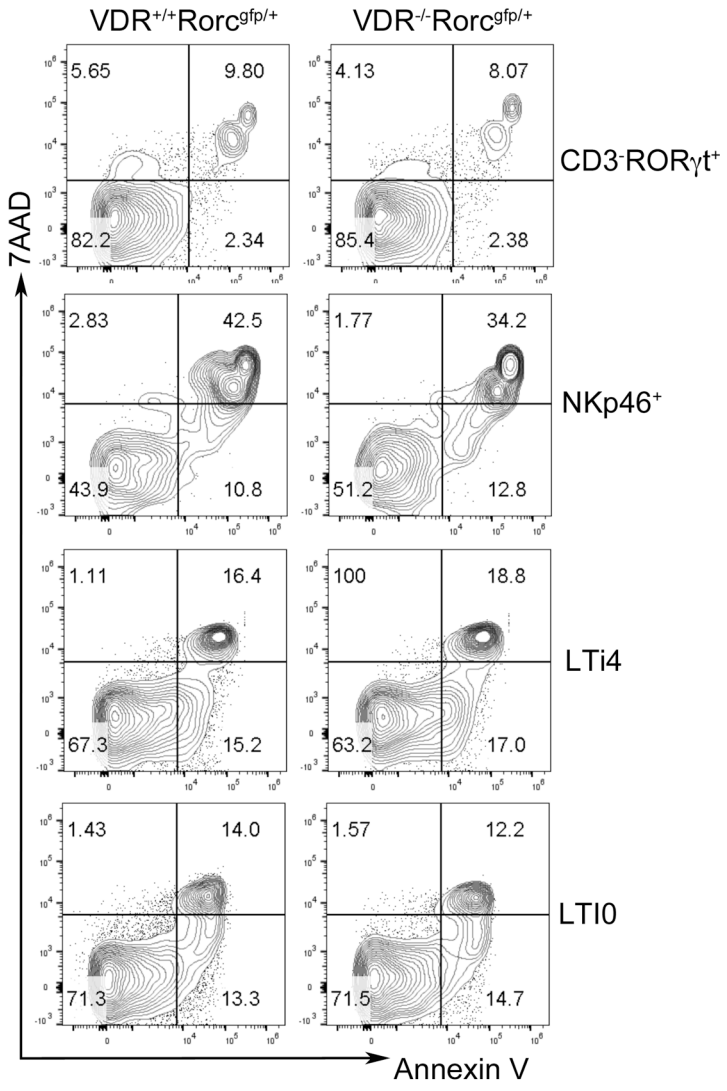

Figure S9. Effects of VDR deletion on gut ILC3 development is independent of ILC3 apoptosis, Related to Figure 6.

Colonic LP cells were isolated from VDR$^{+/+}$Rorc$^{gfp/+}$ and VDR$^{-/-}$Rorc$^{gfp/+}$ mice at steady state, the cells were analyzed for 7AAD and annexin V levels in ILC3 populations. Shown are representative FACS plots for analyses of RORγt^{+}ILC3, NKp46^{+} cells, and LTi4 and LTi0 cells.

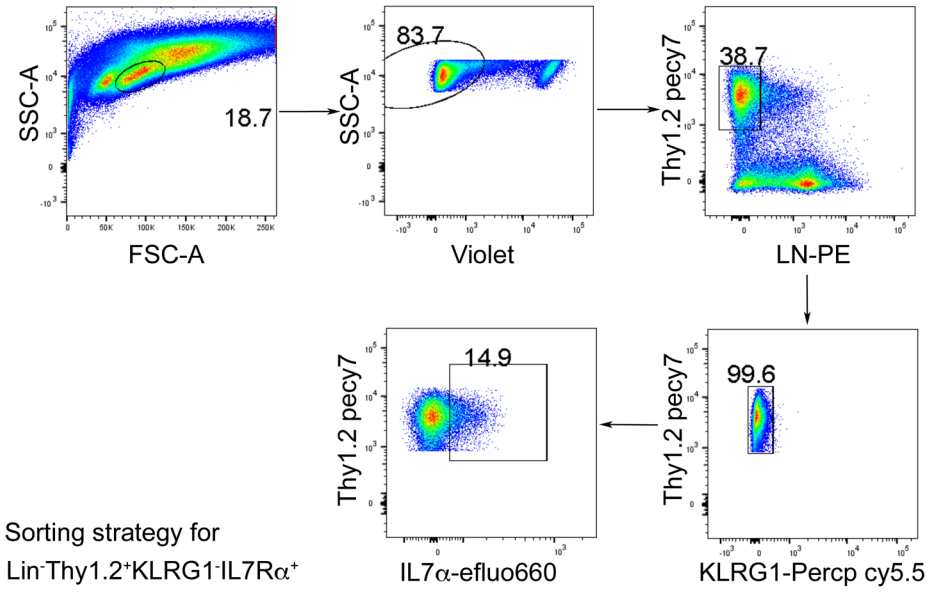

Figure S10. Sorting strategy for Lin$^-$ Thy1.2^{hi}KLRG1$^-$IL-7Rα$^+$ cells from colonic lamina propria cells that were isolated from Rag1$^{-/-}$ mice, Related to Figure 7.

Transparent Methods

Animals

$VDR^{-/-}$ mice were described previously (Li et al., 1997), and $Cyp27b1^{-/-}$ mice that carry a genetic deletion in the 1α-hydroxylase gene (Panda et al., 2001) were obtained from Dr. David Goltzman (McGill University). The $VDR^{-/-}$ and $Cyp27b1^{-/-}$ colonies were maintained on the high calcium/high lactose rescue diet as reported (Li et al., 1998). $VDR^{flox/flox}$ with LoxP sites flanking exon 4 of the *Vdr* gene were reported previously (Chen et al., 2011; He et al., 2018). $Rag1^{-/-}$ mice (Stock #: 002216) that have no mature T and B lymphocytes (Mombaerts et al., 1992), RORγt-EGFP mice ($Rorc^{gfp/+}$, Stock # 007572) that carry EGFP knock-in in the RORγt gene so that RORγt^{+} cells are GFP-positive, and RORγt-Cre transgenic mice (Stock # 022791) that express the Cre recombinase in RORγt-positive cells, were all obtained from Jackson Laboratory. $VDR^{flox/flox}$;RORγt-Cre and $VDR^{-/-}$;$Rag1^{-/-}$ mice were generated by crossing two corresponding strains of mice, respectively. In all studies 6-8 week old mice, both male and female, were used. All animal study protocols were approved by the Institutional Animal Care and Use Committee at the University of Chicago.

Citrobactor rodentium infection

C. rodentium bacteria (Strain DBS100, ATCC 51549) were grown in LB medium at 37°C. Mouse *C. rodentium* infection was carried out based on a method described previously (Koroleva et al., 2015). Mice were orally gavaged with *C. rodentium* at $1x10^{10}$ CFU/mouse suspended in 200 μl PBS for survival studies. For experiments examining ILC3 response, mice were gavaged with *C. rodentium* at $5x10^{9}$ CFU/mouse and killed day 4 or 5. Body weight and death were recorded daily. Feces were collected daily and stored at -80°C for later analyses. To quantify fecal bacteria, feces were weighed and then homogenized in sterile PBS containing 20% glycerol. Serially diluted homogenates were plated on Difco-MacConkey agar (BD Bioscience) plates (Bouladoux et al., 2017). *C. rodentium* colonies were counted after 24 hr incubation at 37°C. To validate the identity of *C. rodentium,* bacterial colonies were randomly picked and bacterial DNA was purified. The DNA was used to amplify the *eae* gene specific to the DBS100 strain (Petty et al., 2010) by PCR, using the following primers: 5'GCCTCCTGTTGCCTGTAG3' (forward) and 5'CCGATCAGAATGGTTATGC3'(reverse). DNA purified from uninfected mouse feces was used as a negative control.

Microbiota depletion

Mouse intestinal commensal bacteria were depleted using antibiotic-induced microbiota-depleted (AIMD) model as described previously (Mukherji et al., 2013; Rakoff-Nahoum et al., 2004). Mice were treated with a cocktail of antibiotics in drinking water (ampicillin 1g/L; vancomycin 500 mg/L; neomycin sulfate 1g/L; and metronidazole 1g/L, all from Sigma-Aldrich) for 4 weeks before being subjected to *C. rodentium* infection. Controls were treated with regular water. To validate the effectiveness of the antibiotic cocktail in gut bacterial depletion, bacterial DNA was purified from fecal pellets from mice with or without this 4-week antibiotic treatment. The DNA was used to PCR-amplify the bacterial 16S rRNA gene using the universal 16S primers: Eub338-5'ACT CCT ACG GGA GGC AGC AG3' (forward) and Eub518-5'ATT ACC GCG GCT GCT GG3' (reverse) based on published work (Fierer et al., 2005).

Bone marrow transplantation

BM transplantation was carried out based on previously published procedure (Szeto et al., 2012). In brief, recipient $Rag1^{-/-}$ mice (6-week old males) were subjected to lethal γ-irradiation (1050 rads, at 200 rads/min), and 6 hours later the mice were transplanted with donor BM cells ($5x10^{6}$ BM cells/mouse) through retra-orbital injection. The donor BM cells were obtained from

$VDR^{flox/flox}$ or $VDR^{flox/flox}$;RORγt-Cre mice. Eight weeks after transplantation, colonic mucosal LP cells were isolated from the recipient mice and ILC3 populations were analyzed by flow cytometry. To validate the success of BM transplantation, in parallel experiments CD45.1 recipient mice were lethally irradiated and transplanted with CD45.2 donor BM cells. Eight weeks after transplantation, the CD45.1 and CD45.2 cell populations in the blood and colonic lamina propria of the recipients were quantified by FACS analysis.

Vitamin D or vitamin D analog treatment

To study the effect of vitamin D on gut ILC3 development, $Cyp27b1^{-/-}$ mice were treated with $1,25(OH)_2D_3$ (AbbVie) at 300 ng/kg (dissolved in 70% propylene glycol) by daily i.p. injection for one week. In another experiment, WT mice were treated with active vitamin D analog paricalcitol (19-nor-1,25-dihydroxyvitamin D_2, AbbVie) at 300 ng/kg (dissolved in 70% propylene glycol) by daily i.p. injection for one week. Controls were treated with 70% propylene glycol vehicle. These treatments did not raise blood calcium levels as reported previously (Zhang et al., 2008; Zhou et al., 2008). After the treatment, colonic LP cells were isolated and subjected to FACS analyses for ILC3 populations.

Lamina propria (LP) cell preparation

LP cells were isolated from the colon as described previously (Zheng et al., 2008). In brief, mice were killed, and the colons were dissected, cut open longitudinally and washed in cold PBS. The colons were cut into 1.5 cm pieces and washed in PBS containing 1 mM DTT for 10 min at room temperature on a shaker, followed by two washes with shaking in PBS containing 30 mM EDTA and 10 mM HEPES at 37°C for 10 min. The tissues were then digested in RPMI 1640 medium containing DNase I (150 μg/ml, Sigma-Aldrich) and collagenase VIII (150 U/ml, Sigma-Aldrich) with 10% fetal bovine serum at 37°C in a 5% CO_2 incubator for 1.5 hrs. Digested cell suspensions were passed through a 70 μm cell strainer and separated by centrifugation on a discontinuous 40%/80% Percoll gradient at 2500 rpm for 20 min at room temperature. Cells were then harvested for flow cytometric analyses.

Flow cytometry

Flow cytometric analysis was performed as described previously (Shi et al., 2016). Non-specific binding to Fc receptors was blocked with anti-CD16/32 antibody (eBioscience) before cell surface staining. For intracellular staining, cells were fixed and permeablized using a Mouse Regulatory T Cell Staining Kit (eBioscience). For cytokine production, cells were stimulated with PMA (50 ng/ml) and ionomycin (500 ng/ml) for 4 hrs. Brefeldin A (2 μg/ml) was added 2 hrs before cells were harvested for analysis. Dead cells were excluded from the analysis using a Live and Dead Violet Viability Kit (Invitrogen**).** ILC3 was defined as $CD3^-ROR\gamma t^+$, $NKp46^+$ cells as $CD3^-ROR\gamma t^+NKp46^+$, LTi0 cells as $CD3^-ROR\gamma t^+NKp46^-CD4^-$ and LTi4 cells as $CD3^-ROR\gamma t^+NKp46^-CD4^+$. Antibodies used in flow cytometric analyses as follows: anti-CD3e-FITC (clone 145-2C11, Biolegend), anti-CD4-Pecy7 (clone RM4-4, Biolegend), anti-NKp46-Percp-Cy5.5 (clone 29A1.4, Biolegend), anti-RORγt-PE (clone AFKJS-9, eBioscience), anti-IL-22-APC (clone IL22JOP, eBioscience), anti-Ki67-eFluor660 (clone SolA15, eBioscience), anti-CD103-APC (clone 2E7, eBioscience), anti-CD45.1-FITC (clone A20, Biolegend), and anti-CD45.2-PE (clone 104, Biolegend). Cell apoptosis detection with Annexin V-7AAD staining was performed using the Annexin V Apoptosis Detection Kit from BD Biosciences (#559763). Fluorescence-activated cell sorting (FACS) was performed in a BD LSRFortessa unit (BD Biosciences) and data analyzed by FlowJo software V10 (Tree Star Inc).

In vitro ILC3 proliferation

Colonic LP cells were prepared from $Rag1^{-/-}$ mice and Lin^{-}(CD11c, CD11b, CD3, CD19, B220, NK1.1, TER119, Ly6G)$Thy1.2^{hi}KLRG1^{-}IL\text{-}7R\alpha^{+}$ cells were sorted by FACS as described previously (Spencer et al., 2014), using a BD FACSAria Fusion unit (BD Biosciences). These cells were then cultured at $1x10^4$ cells/well in 50 μl RPMI 1640 supplemented with 10% FBS, 1x penicillin/streptomycin, non-essential amino acids, β-mercaptoethanol (50 mM), IL-7 (10 ng/ml, Biolegend) and SCF (10 ng/ml, Biolegend) in the presence or absence of $1,25(OH)_2D_3$ (20 nM). After 3 days of culture, $Ki67^{+}ROR\gamma t^{+}$ cell populations were quantified by FACS analysis. The antibodies used in the sorting were as follows: anti-CD11c-PE (clone N418, eBioscience), anti-CD11b-PE (clone M1/70, Biolegend), anti-CD3-PE (clone 145-2C11, Biolegend), anti-B220-PE (clone RA3-6B2, eBioscience), anti-NK1.1-PE (clone PK136, BD Biosciences), anti-TER119-PE (clone TER-119, eBioscience), anti-Ly6G-PE (clone RB6-8C5, eBioscience), anti-Thy1.2-Pecy7 (CD90.2) (clone 53-2.1, eBioscience), anti-KLRG-PercpCy5.5 (clone 2F1, BD Biosciences), anti-IL-7Rα-efluo660 (CD127) (clone A7R34, eBioscience).

Statistical analysis

Data values were presented as means ± SEM. Statistical comparisons were carried out using unpaired two-tailed Student's *t*-test for two group comparisons, and for three or more group comparisons two-way analysis of variance (ANOVA) was used with a Student-Newman-Keuls post-hoc test. Animal body weight changes and survival rate were analyzed by log-rank test. $P< 0.05$ were considered statistically significant.

Supplemental References

Bouladoux, N., Harrison, O.J., and Belkaid, Y. (2017). The Mouse Model of Infection with Citrobacter rodentium. Curr Protoc Immunol *119*, 19 15 11-19 15 25.

Chen, S., Law, C.S., Grigsby, C.L., Olsen, K., Hong, T.T., Zhang, Y., Yeghiazarians, Y., and Gardner, D.G. (2011). Cardiomyocyte-specific deletion of the vitamin D receptor gene results in cardiac hypertrophy. Circulation *124*, 1838-1847.

Fierer, N., Jackson, J.A., Vilgalys, R., and Jackson, R.B. (2005). Assessment of soil microbial community structure by use of taxon-specific quantitative PCR assays. Appl Environ Microbiol *71*, 4117-4120.

He, L., Liu, T., Shi, Y., Tian, F., Hu, H., Deb, D.K., Chen, Y., Bissonnette, M., and Li, Y.C. (2018). Gut Epithelial Vitamin D Receptor Regulates Microbiota-Dependent Mucosal Inflammation by Suppressing Intestinal Epithelial Cell Apoptosis. Endocrinology *159*, 967-979.

Koroleva, E.P., Halperin, S., Gubernatorova, E.O., Macho-Fernandez, E., Spencer, C.M., and Tumanov, A.V. (2015). Citrobacter rodentium-induced colitis: A robust model to study mucosal immune responses in the gut. J Immunol Methods *421*, 61-72.

Li, Y.C., Amling, M., Pirro, A.E., Priemel, M., Meuse, J., Baron, R., Delling, G., and Demay, M.B. (1998). Normalization of mineral ion homeostasis by dietary means prevents hyperparathyroidism, rickets, and osteomalacia, but not alopecia in vitamin D receptor-ablated mice. Endocrinology *139*, 4391-4396.

Li, Y.C., Pirro, A.E., Amling, M., Delling, G., Baron, R., Bronson, R., and Demay, M.B. (1997). Targeted ablation of the vitamin D receptor: an animal model of vitamin D-dependent rickets type II with alopecia. Proc Natl Acad Sci U S A *94*, 9831-9835.

Mombaerts, P., Iacomini, J., Johnson, R.S., Herrup, K., Tonegawa, S., and Papaioannou, V.E. (1992). RAG-1-deficient mice have no mature B and T lymphocytes. Cell *68*, 869-877.

Mukherji, A., Kobiita, A., Ye, T., and Chambon, P. (2013). Homeostasis in Intestinal Epithelium Is Orchestrated by the Circadian Clock and Microbiota Cues Transduced by TLRs. Cell *153*, 812-827.

Panda, D.K., Miao, D., Tremblay, M.L., Sirois, J., Farookhi, R., Hendy, G.N., and Goltzman, D. (2001). Targeted ablation of the 25-hydroxyvitamin D 1alpha -hydroxylase enzyme: evidence for skeletal, reproductive, and immune dysfunction. Proc Natl Acad Sci U S A *98*, 7498-7503.

Petty, N.K., Bulgin, R., Crepin, V.F., Cerdeno-Tarraga, A.M., Schroeder, G.N., Quail, M.A., Lennard, N., Corton, C., Barron, A., Clark, L., et al. (2010). The Citrobacter rodentium genome sequence reveals convergent evolution with human pathogenic Escherichia coli. J Bacteriol *192*, 525-538.

Rakoff-Nahoum, S., Paglino, J., Eslami-Varzaneh, F., Edberg, S., and Medzhitov, R. (2004). Recognition of commensal microflora by toll-like receptors is required for intestinal homeostasis. Cell *118*, 229-241.

Shi, Y., Liu, T., He, L., Dougherty, U., Chen, L., Adhikari, S., Alpert, L., Zhou, G., Liu, W., Wang, J., et al. (2016). Activation of the Renin-Angiotensin System Promotes Colitis Development. Sci Rep *6*, 27552.

Spencer, S.P., Wilhelm, C., Yang, Q., Hall, J.A., Bouladoux, N., Boyd, A., Nutman, T.B., Urban, J.F., Jr., Wang, J., Ramalingam, T.R., et al. (2014). Adaptation of innate lymphoid cells to a micronutrient deficiency promotes type 2 barrier immunity. Science *343*, 432-437.

Szeto, F.L., Reardon, C.A., Yoon, D., Wang, Y., Wong, K.E., Chen, Y., Kong, J., Liu, S.Q., Thadhani, R., Getz, G.S., et al. (2012). Vitamin D receptor signaling inhibits atherosclerosis in mice. Mol Endocrinol *26*, 1091-1101.

Zhang, Z., Zhang, Y., Ning, G., Deb, D.K., Kong, J., and Li, Y.C. (2008). Combination therapy with AT1 blocker and vitamin D analog markedly ameliorates diabetic nephropathy: blockade of compensatory renin increase. Proc Natl Acad Sci U S A *105*, 15896-15901.

Zheng, Y., Valdez, P.A., Danilenko, D.M., Hu, Y., Sa, S.M., Gong, Q., Abbas, A.R., Modrusan, Z., Ghilardi, N., de Sauvage, F.J., et al. (2008). Interleukin-22 mediates early host defense against attaching and effacing bacterial pathogens. Nature medicine *14*, 282-289.

Zhou, C., Lu, F., Cao, K., Xu, D., Goltzman, D., and Miao, D. (2008). Calcium-independent and 1,25(OH)2D3-dependent regulation of the renin-angiotensin system in 1alpha-hydroxylase knockout mice. Kidney Int *74*, 170-179.